

## NOTICE

THIS DOCUMENT HAS BEEN REPRODUCED FROM  
MICROFICHE. ALTHOUGH IT IS RECOGNIZED THAT  
CERTAIN PORTIONS ARE ILLEGIBLE, IT IS BEING RELEASED  
IN THE INTEREST OF MAKING AVAILABLE AS MUCH  
INFORMATION AS POSSIBLE

(NASA-CR-162929) STUDY OF WRAP-RIB ANTENNA  
DESIGN Final Report (Lockheed Missiles and  
Space Co.) 85 p HC A05/MF 801 CSCL 09C

N80-22544 3

1979

Unclassified

G3/32 17250

FINAL REPORT  
FOR  
STUDY OF WRAP-RIB ANTENNA DESIGN

CONTRACT NUMBER 955345

*Prepared For*

## JET PROPULSION LABORATORY

**CALIFORNIA INSTITUTE OF TECHNOLOGY**

Pasadena, California 91730



"This work was performed for the Jet Propulsion Laboratory, California Institute of Technology sponsored by the National Aeronautics and Space Administration under contract NAS7-100."

**LOCKHEED MISSILES & SPACE COMPANY, INC.**  
**SPACE SYSTEMS DIVISION • SUNNYVALE, CALIFORNIA**

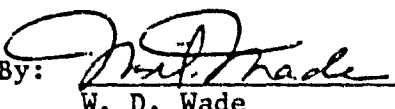
LMSC-D714613  
12 December 1979

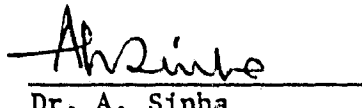
Final Report  
for  
STUDY OF WRAP-RIB ANTENNA DESIGN

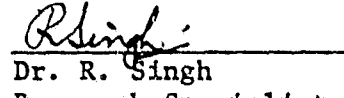
Contract Number 955345

Prepared For  
JET PROPULSION LABORATORY  
CALIFORNIA INSTITUTE OF TECHNOLOGY  
Pasadena, California 91730

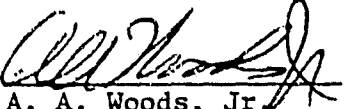
Prepared By:

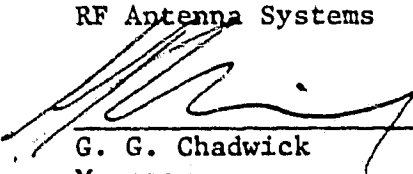
  
W. D. Wade  
Design Specialist  
RF Antenna Systems

  
Dr. A. Sinha  
Design Specialist  
RF Antenna Systems

  
Dr. R. Singh  
Research Specialist  
RF Antenna Systems

Approved By:

  
A. A. Woods, Jr.  
Supervisor  
RF Antenna Systems

  
G. G. Chadwick  
Manager  
RF Antenna Systems

"This work was performed for the Jet Propulsion Laboratory, California Institute of Technology sponsored by the National Aeronautics and Space Administration under contract NAS7-100."

This report contains information prepared by Lockheed Missiles and Space Company, Inc., under JPL sub-contract. Its content is not necessarily endorsed by the Jet Propulsion Laboratory, California Institute of Technology, or the National Aeronautics and Space Administration

The appendices referenced in this report can be obtained by formal request.

## ABSTRACT

This final report presents the results of a parametric design study which was conducted to develop the significant characteristics and technology limitations of space deployable antenna systems with aperture sizes ranging from 50 up to 300 m and F/D ratios between 0.5 and 3.0. This study considered the Lockheed Missiles and Space Company, Inc. wrap-rib type reflectors of both the prime and offset fed geometry and associated feed support structures.

The significant constraints investigated as limitations on achievable aperture were inherent manufacturability, orbit dynamic and thermal stability, antenna weight and antenna stowed volume. A portion of the study identified the maximum number of ribs and aperture size considering the limitations imposed by STS stowage volume and weight for a wrap-rib reflector. The orbital thermal environment and approximation error was then considered to identify the maximum operational frequency for reflector efficiencies on the order of 85%. These results were used to form the data base resulting in the defined maximum achievable aperture size as a function of diameter, frequency and estimated cost.

## TABLE OF CONTENTS

<u>Section</u>		<u>Page</u>
ABSTRACT .....		iii
LIST OF FIGURES .....		vii
SUMMARY .....		ix
1 INTRODUCTION .....		1
2 TECHNICAL DISCUSSION .....		2
2.1 Antenna Geometry and Design Approach Overview ..		2
2.1.1 Selection of Offset Antenna Design		
Approach .....		5
2.1.2 Wrap Rib Geometry .....		9
2.1.3 Feed Support Structure .....		19
2.1.4 System Ascent and Deployment .....		28
2.2 Performance Model .....		30
2.2.1 Design Package Computer Program .....		35
2.2.2 Analytical Description of an Offset		
Wrap Rib Reflector .....		39
2.2.3 Thermal Distortion Analysis .....		39
2.3 Performance Projections .....		43
2.3.1 Weight Impact on Aperture Size .....		43
2.3.2 STS Stowed Volume .....		45
2.3.3 Surface Figure Considerations .....		46

## TABLE OF CONTENTS (Continued)

<u>Section</u>		<u>Page</u>
2.3.4	Sensitivity to Design Parameters .....	52
2.3.5	Projected Antenna Costs .....	56
2.4	Program Plan .....	58
2.4.1	55-Meter-Diameter Model Design .....	60
2.4.2	55-Meter-Diameter Reflector Test Equipment .....	63
2.4.3	Reflector Model Fabrication and Assembly .....	65
2.4.4	55-Meter-Diameter Reflector Model Implementation Schedule .....	66
3	CONCLUSIONS .....	71
4	RECOMMENDATIONS .....	73
5	NEW TECHNOLOGY .....	74
APPENDICIES		
A -	Antenna Design Package Computer Program Listing .	A-1
B -	Antenna Thermal Distortion Analysis .....	B-1
C -	Temperature Distribution in Closed Lenticular Rib Sections .....	C-1
D -	Reflector Distortion Analysis .....	D-1

## TABLE OF CONTENTS (Continued)

<u>Section</u>		<u>Page</u>
E - Derivation for Lenticular Cross Sectional Properties .....		E-1
F - Computation of RMS of Offset Reflector .....		F-1

## LIST OF FIGURES

<u>Number</u>		<u>Page</u>
1	Typical Axi-Symmetric Parabolic Antenna System .....	2
2	Symmetric Wrap-Rib Reflector Concept .....	3
3	Redeployable Mast .....	4
4	Offset Reflector Geometry .....	5
5	Stowed Offset Fan-Flex Antenna .....	6
6	Deployed Fan-Flex During Range Testing .....	7
7	Offset Wrap-Rib Design Approach .....	8
8	Lenticular Rib Cross Section .....	10
9	GR/E Rib Mounted Cup-Down .....	11
10	GR/E Rib Mounted Cup-Up .....	11
11	Moly/Gold Knit Mesh .....	14
12	Stowed Configuration .....	16
13	Hub Section and Drive System .....	17
14	Rib Adjustment Mechanism .....	18
15	Feed Support Structure Surveyed .....	20
16	Mast Collapsing Member .....	25
17	Mast Section Stowing Sequence .....	26
18	Offset Fed Antenna System Operational Sequence .....	28
19	Modeling Approach .....	30
20	Analysis/Computer Flow Chart .....	32
21	Antenna Optimization Package Overview .....	34
22	Example of Summary Output .....	36

## LIST OF FIGURES (Continued)

<u>Number</u>		<u>Page</u>
23	Example of Detail Output .....	40
24	Thermal Model Geometry .....	42
25	Upper Limit of Surface Quality .....	44
26	Weight Constrained Aperture Limits .....	44
27	Antenna Systems Stowed Length Requirements .....	45
28	Surface Figure of STS Diameter Constrained Symmetric Antenna .....	46
29	Surface Figure of STS Diameter Constrained Offset Antenna .....	47
30	Synchronous P/L Surface Characteristics for a Symmetric Antenna .....	48
31	Synchronous P/L Surface Characteristics for an Offset Antenna .....	49
32	Synchronous Component Surface Characteristics for a Symmetric Antenna .....	50
33	Synchronous Component Surface Characteristics for an Offset Antenna .....	51
34	Antenna System Sensitivity to F/D for an Offset Antenna .....	52
35	Antenna Sensitivity to Material Characteristics .....	53
36	Surface Figure Characteristics with Metal Matrix Ribs	54
37	Antenna System Sensitivity to Rib Design .....	55
	viii	

## LIST OF FIGURES (Continued)

<u>Number</u>		<u>Page</u>
38	Offset Antenna Cost Projections .....	56
39	Offset Vs. Symmetric Antenna Cost Comparison .....	57
40	Lenticular Rib Splice Details .....	62
41	Gold Plated Molybdenum Wire Mesh .....	64
42	55-Meter-Diameter Reflector Model Implementation Schedule .....	67

## SUMMARY

The "Study of Wrap-Rib Antenna Design" was conducted to determine the applicability of the design for offset feed configurations in terms of surface quality, cost, weight mechanical complexity and deployable feed support structures for antennas up to 300 m in diameter. This activity was accomplished by constructing an analytical model of the reflector and feed support structure which developed detailed designs and performance projections compatible with ascent system constraints and the fundamental material property and geometry constraints of the designs. Execution of the developed model allowed the generation of the reference data for the definition of the desired performance characteristics as a function of aperture diameter.

The study identified that for the reflector the dominant errors, thus the performance limiting errors, were those of thermal distortion and surface approximation. All other error sources were shown to be an order of magnitude less significant. The feed support structure did not limit the antenna performance due to feed induced beam shift until the focal length was increased to about three times the actual section diameter for the offset geometry. The symmetric geometry was not feed structure limited within the scope of the parameters investigated. At no time in the investigation were the Shuttle Transportation System volume or weight constraints found to be the driving constraints on the achievement of the large aperture systems design.

As with any study one must be conservative when drawing conclusions. With this conservatism in mind the following conclusions can be drawn from the results:

- o Offset wrap rib antennas up to 150 m diameter are feasible for operation at 2 to 3 GHz.
- o STS compatibility is not a design driver.
- o Cost and technical risks indicate a new data base of about 50 M required prior to undertaking 100 to 150 m designs.
- o Further activity should include active surface control and control systems interaction studies.

It is hoped that further activity will define the reasonableness of designs which are at the actual limits of the technical work performed - 300 m deployable antennas!

SECTION 1  
INTRODUCTION

This final report contains a summary of the technical activity accomplished under "Study of Wrap-Rib Antenna Design" for The Jet Propulsion Laboratory, California Institute of Technology. The study activity was specifically undertaken to identify the significant characteristics and technology limitations of wrap-rib concept space deployable antenna systems as the design is allowed to grow in size until constrained by known technology. Practical considerations such as ground testability, facility requirements, manufacturing techniques, etc. were intentionally not used as constraints but addressed via the development of a program plan. This program plan defines a logical, low risk approach toward the evolution of the projected designs and a timely removal of significant risk prior to a flight experiment.

The specific technical tasks performed in support of this contract and reported herein were to (a) define the wrap rib antenna design for both symmetric and offset configurations in terms of surface quality, cost, weight and mechanical complexity, (b) develop a supporting deployable feed support structure and characterize it in terms of performance impact, cost, weight and mechanical complexity, and (c) develop a technical approach for implementation consisting of a combination of analysis and component test, model testing, and possibly space flight hardware demonstrations.

SECTION 2  
TECHNICAL DISCUSSION

2.1 ANTENNA GEOMETRY AND DESIGN APPROACH OVERVIEW

To date the large antenna systems are most commonly constructed as symmetric parabolic reflector systems. This geometry is shown in Figure 1.

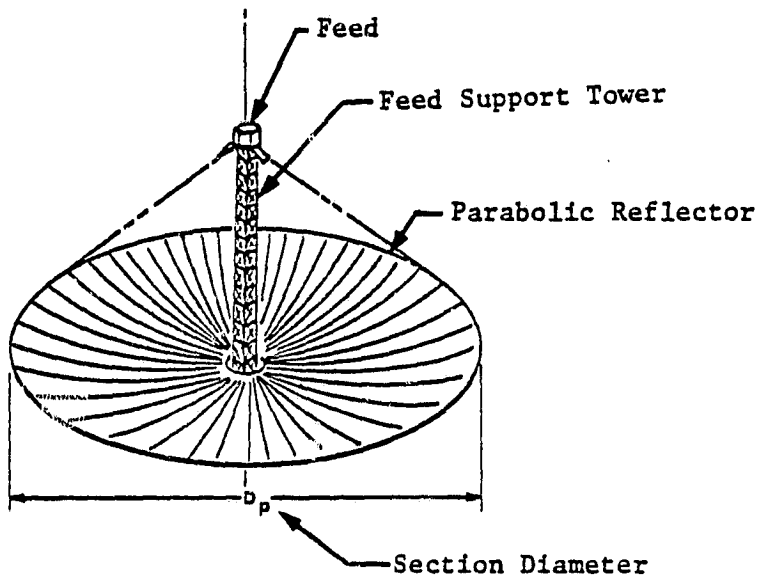


Figure 1. Typical Axi-Symmetric Parabolic Antenna System

The axi-symmetric, deployable wrap-rib parabolic reflector is based on an approximation to a paraboloid of revolution. The wrap-rib antenna is comprised of radially emanating gores between the ribs which take the form of parabolic cylinders. The parabolic cylinders more closely approximate a true paraboloid of revolution as the number of gores is increased. The point of diminishing returns for this reflector in terms of antenna performance is a function of both the radio frequency

wavelength of interest and the reflector diameter. Figure 2 illustrates the physical appearance of the resulting reflector.

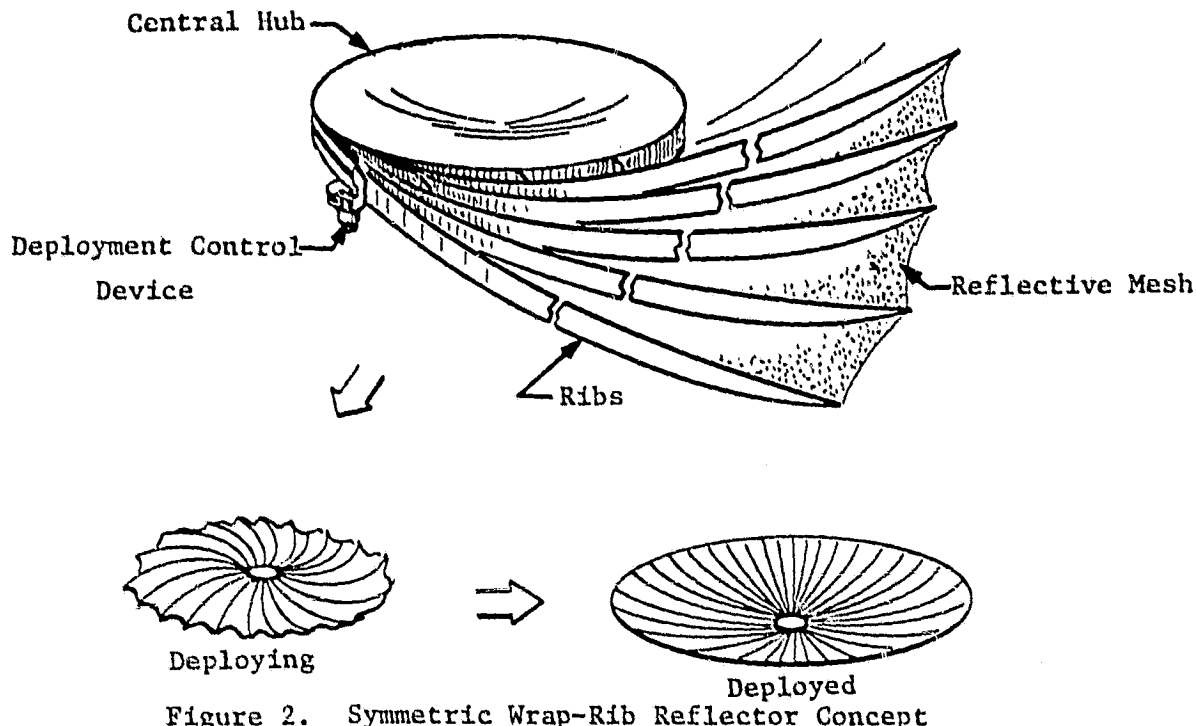


Figure 2. Symmetric Wrap-Rib Reflector Concept

The gores are fabricated from a flexible membrane material which is usually a knitted or woven fabric of electrically conductive material. The gores are sewn to parabolically curved cantilevered ribs terminated at the central hub structure in a hinge fitting. For launch the antenna must be folded into a package size which will fit into the Shuttle Transportation System. For stowage the ribs are rotated on the hinge pin, then elastically buckled and wrapped around the hub. Once in space, the reflector is deployed by a deployment restraint mechanism which simply controls the rate of energy release and therefore the deployment rate.

The key elements in the feed support tower are the three lenticular shaped longitudinal members which can support an appreciable load when erect, but which can be folded upon themselves through the application of lateral and axial forces. For resisting torsional and lateral shear

forces, wire tension cables are provided. The battens are necessary for supporting section hinges and for resisting the lateral, destabilizing cable reactions.

Figure 3 shows the overall mast system and emphasizes the stowage and deployment systems. The inner system performs the actual, section-by-section deployment and retraction of the mast through the use of three synchronous motor, sprocket, chain and development cog systems. It also serves as the bottom mast section until that section, itself, is fully erect.

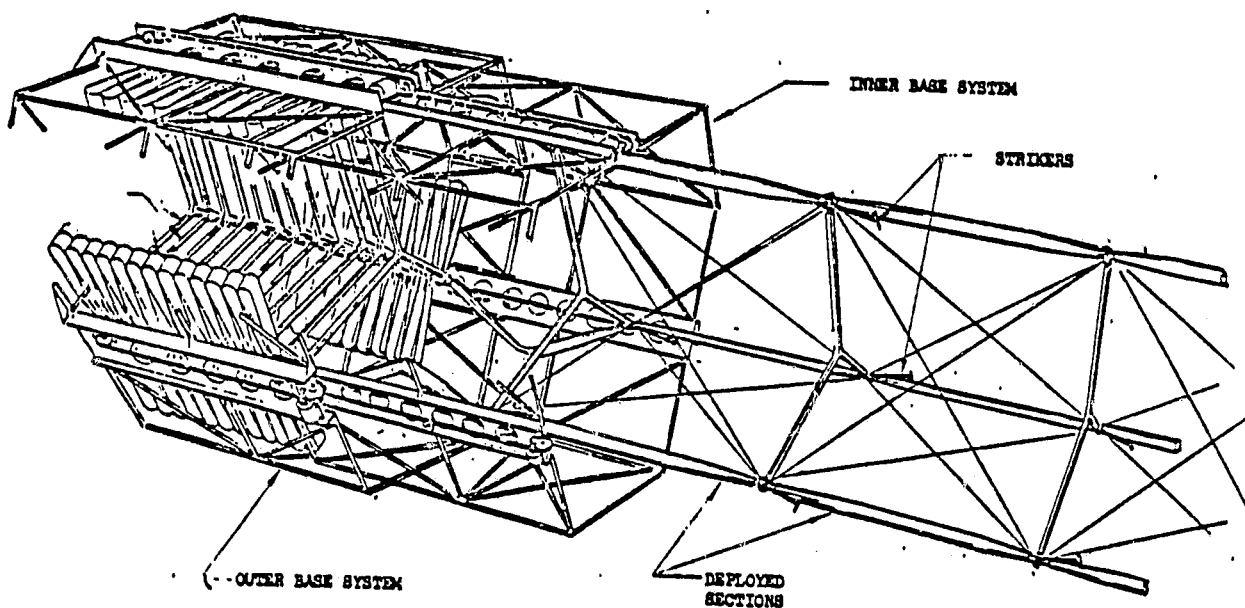


Figure 3. Redeployable Mast

### 2.1.1 Selection of Offset Antenna Design Approach

Geometrically an offset reflector is described by a paraboloid where the geometric centerline is not coincident with the parabolic axis of symmetry. In order to gain the electrical advantages of reduced blockage the parabolic axis and therefore the focal point must in fact be located external to the section aperture. This section can most easily be visualized by forming a large paraboloid of diameter  $D$  and then passing a cylinder, with a parallel axis of symmetry, through the paraboloid (Figure 4). If the cylinder has a diameter ( $d$ ) less than  $D/2$  and its radius is common with the radius of the parabola, the section of the paraboloid bounded by the cylinder is representative of the desired offset reflector surface. Further if  $D/2-d$  is larger than the radius of the feed and the feed support structure is attached external to the radius of the offset section there is no blockage of the electrical field of view.

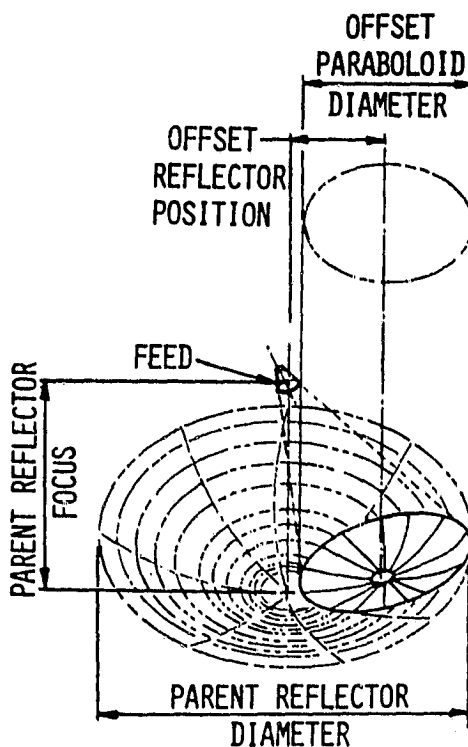


Figure 4. Offset Reflector Geometry

This new surface can be described mathematically with a simple coordinate transformation and rotation of the equations for the parent paraboloid. The result is a planar symmetric structure as opposed to the original axisymmetric structure with impacts in manufacturing and assembly costs due to the added geometrical complexity.

As a result of the manufacturing considerations the initial adaptation of the wrap-rib design for use as an offset paraboloid retained as much of the structural symmetries as possible. In fact, the reflector section was constructed as a section of the parent parabola. This design, known as the fan-flex, was fabricated and tested in 1975. Figure 5 presents a picture of a stowed antenna system containing two deployable fan-flex reflectors and Figure 6 shows the system deployed during range testing.

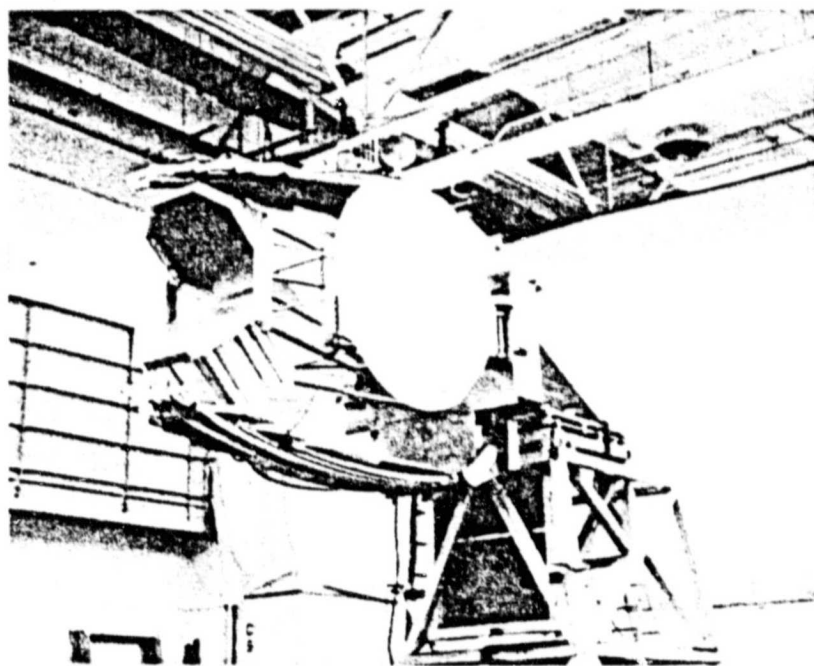


Figure 5. Stowed Offset Fan-Flex Antenna

ORIGINAL PAGE IS  
OF POOR QUALITY

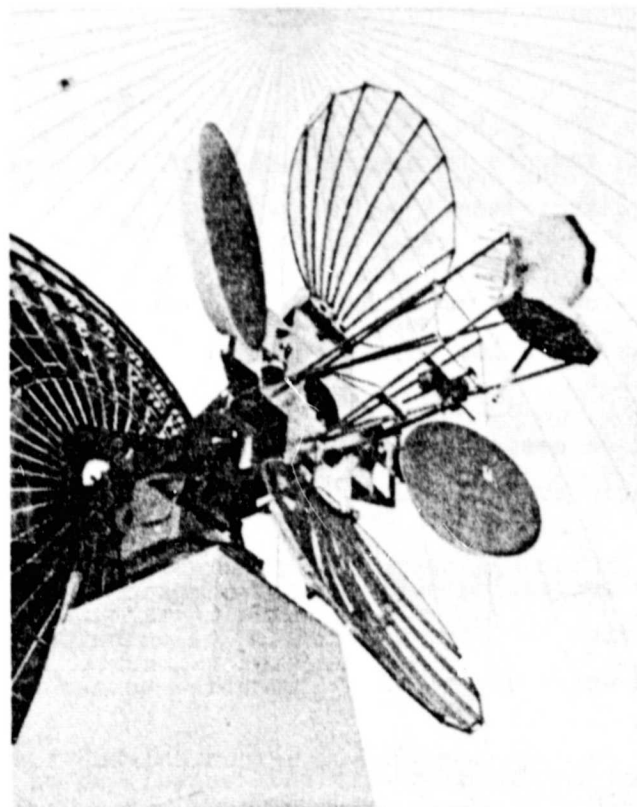


Figure 6. Deployed Fan-Flex During Range Testing

The fan-flex, although successful in the aforementioned design application presented some serious growth limitations. These were a large stowed envelope relative to the wrap-rib, a long and therefore heavy rib since the rib was edge mounted and had to be designed for ascent loading, and a surface approximation ill-conditioned to the illumination function of the surface. The end result was a design with limited growth compared to the wrap-rib from a size and weight standpoint.

The logical design solution was to adapt the wrap-rib and minimize the cost impact in the manufacturing and assembly areas. The offset wrap-rib, shown in Figure 7, uses the radial rib system attached to a central hub as in the axisymmetric design except that the hub is now located in the center of the offset section with the plane of the hub parallel to the local slope of the section. The significant benefits of the adaptation are:

- o Rib length is reduced to approximately  $D/2$  which reduces weight and thermal distortions.
- o Ribs can be wrapped around the central hub for storage during ascent preserving a low volume package.
- o Rib and surface designs developed and proven with the axisymmetric wrap-rib are useable.
- o The radially increasing surface approximation error is well conditioned with the offset reflector illumination function distribution which minimizes the required number of ribs.
- o A shaped cover can be used over the central hub to preserve the surface contour.

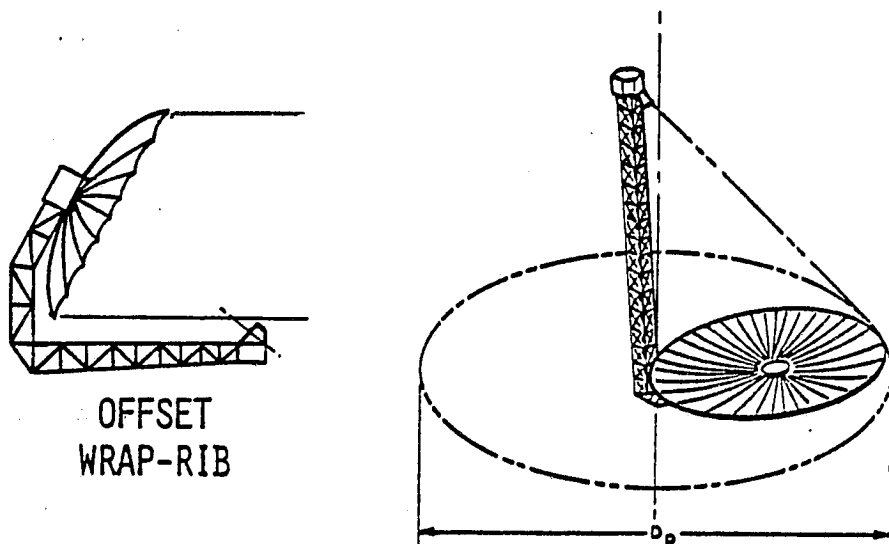


Figure 7. Offset Wrap-Rib Design Approach

### 2.1.2 Wrap Rib Overview

The wrap-rib design concept consists of a number (variable) of radial ribs or beams which are cantilevered from a central hub structure. Each of the ribs is attached to this hub through hinges. The radial spoke system provides the mounting for the antenna structure. For parabolic or other curved reflectors, the ribs are formed in the required shape, and reflective pie-shaped gores are attached between the ribs.

The rib cross section and material are chosen to permit the elastic buckling of the ribs. This is to allow the ribs to be wrapped around the hub structure in the ascent or stowed package configuration.

In the stowing process, the ribs and attached surface are rotated about the rib hinges until the ribs are tangent to the hub. After this rotation, the ribs are pulled around the hub and are wrapped up. The elastic buckling of each rib accommodates this action. The surface material is allowed to form a package between the ribs.

The elastic energy stored in the wrapped ribs is sufficient to accomplish deployment of relatively small (less than 20 m) diameter systems. In this case, the stowed package is contained by a series of hinged doors which are held in place by a restraining cable. Deployment occurs when the cable is severed. For the larger diameters, the surface loads and momentum exchange with the spacecraft will not allow this free deployment. A deployment restraint system has been incorporated in the design to control this sudden release of strain energy.

## 2.1.2.1 Ribs

Graphite epoxy was chosen as the rib material due to the inherently low coefficient of thermal expansion that can be achieved. The particular material composition and orientation selected is the Fiberite Company is 0.005 inch HMS/34 tape in a (0°/90°/90°/0°) laminate. The properties of these lamina materials and the resulting composite laminate are listed in Table I.

The cross section designed for this rib is shown in Figure 8. For comparison purposes, the photographs in Figures 9 and 10 are of the ribs fabricated during Independent Research and Development activities.

Mesh attachment is provided for by the addition of hollow eyelets installed near the parabolic edge of the rib. The purpose of these eyelets is to protect the sewing thread from the chaffing that would result from bare graphite epoxy holes.

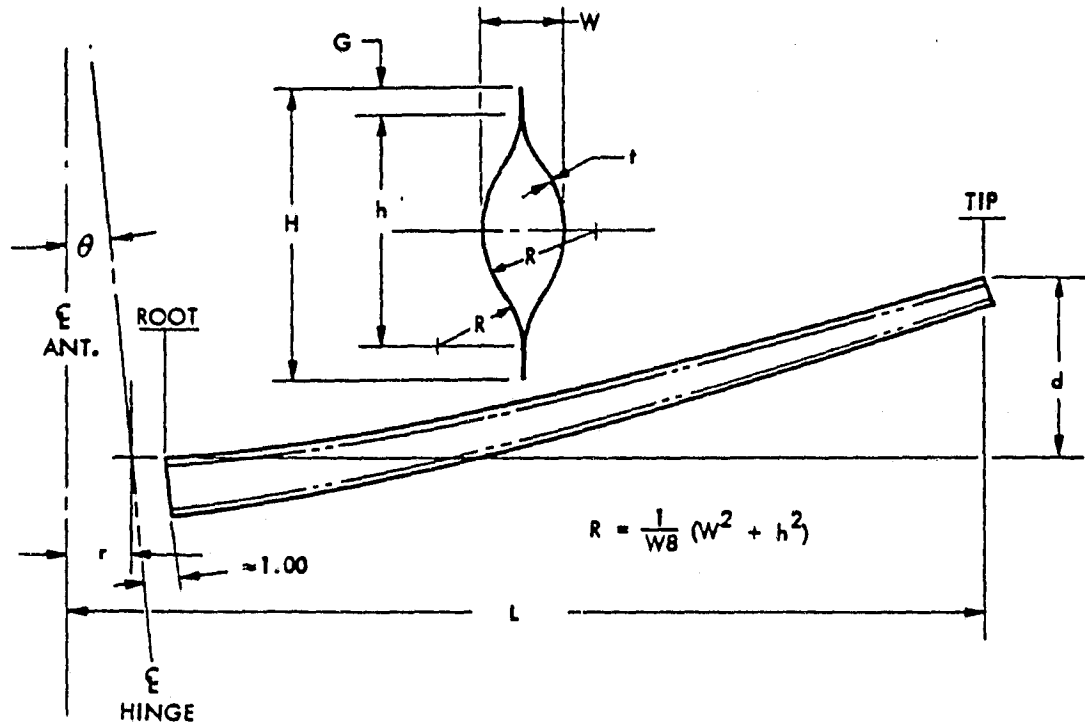


Figure 8. Lenticular Rib Cross Section

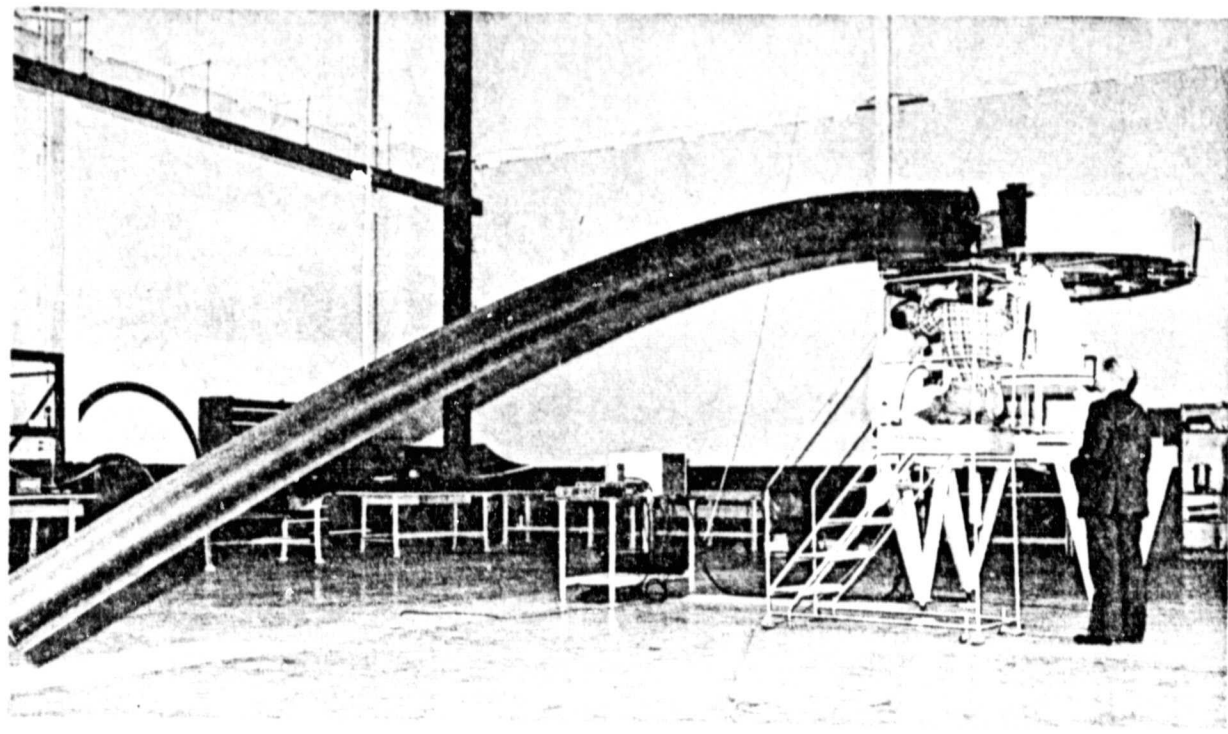


Figure 9. GR/E Rib Mounted Cup-Down

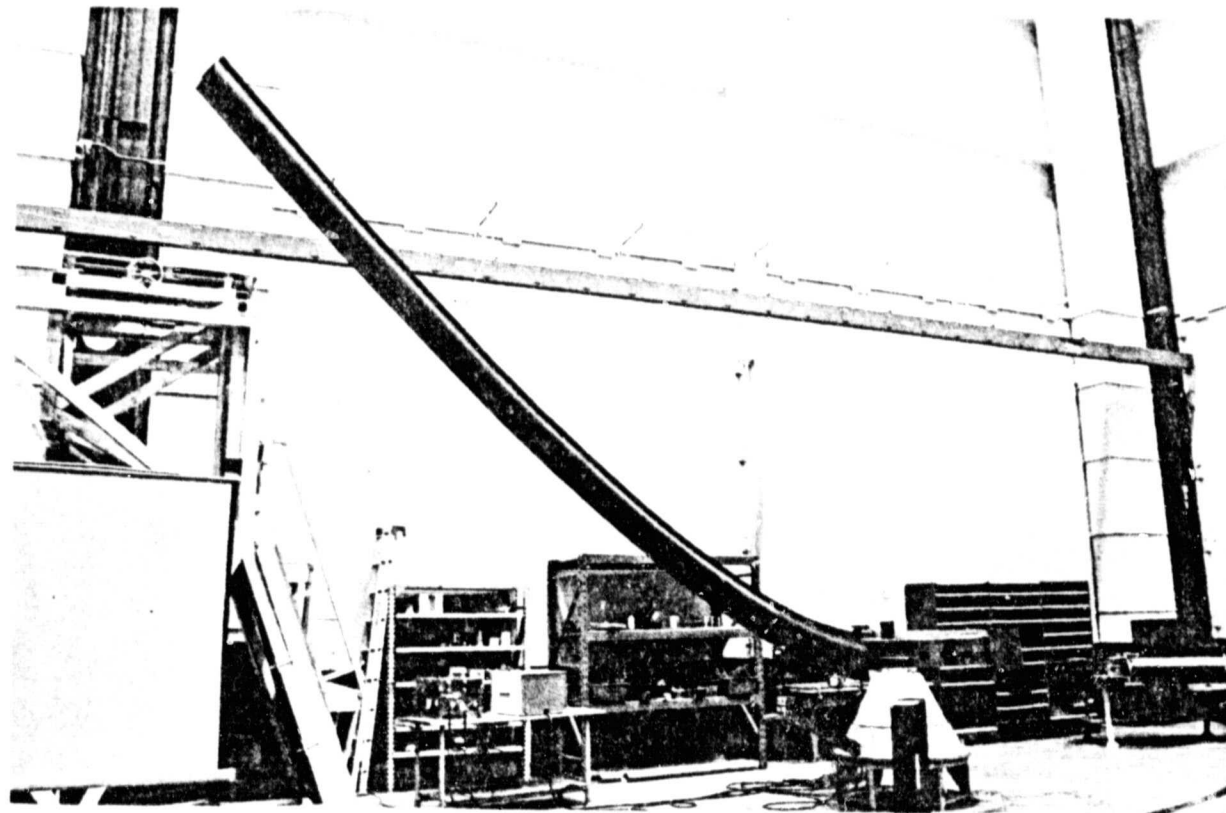


Figure 10. GR/E Rib Mounted Cup-Up

Table 1. Material Properties Of Layup Configurations

Parameter	HMS/HMS/HMS (0/90 <sub>2</sub> /0)
Young's Modulus (msi)	14.0
Shear Modulus (msi)	0.60
Thermal Coefficient of Expansion ( $\times 10^{-6}/^{\circ}\text{F}$ )	0.1
Ultimate Tensile Strength (ksi)	57.0
Ultimate Compressive Strength (ksi)	51.0
Thermal Conductivity (Btu/hr-ft- $^{\circ}\text{F}$ )	13.6

### 2.1.2.2 Mesh

The rf reflective surface or mesh that is stretched between the radial ribs is fabricated on a two bar, tricot knit machine, from 0.0012 inch diameter gold plated molybdenum wire. The resulting mesh is similar to that shown in Figure 11. The mechanical thermal and optical properties for this particular mesh material are estimated from three known, tested data points.

The reflection coefficient of a given knitted tricot mesh can be estimated using the following relationship:

$$R = \frac{1}{1 + 4 \left[ \frac{S \times \ln \left[ \frac{S}{3\pi d} \right]}{\lambda} \right]^2}$$

where:  $S$  = Cell spacing/in  
 $\lambda$  = rf wavelength  
 $d$  = Wire diameter

For the parametric analysis, a reflectivity of 95% was chosen and the corresponding cell spacing was calculated from the relationship. A best fit equation through the three known mesh stiffness data points was derived. This allowed the mesh properties to vary as a function of rf frequency.

Fabrication of mesh gores is accomplished with the aid of a preload vibration table. The mesh is rolled out onto a cutting table the surface of which has been marked with the gore cut line. Weights of the appropriate value are attached to the periphery. The table is vibrated to allow the mesh to reposition itself into a uniform load condition. Strip magnets are placed along the cut line. Kevlar tape is bonded at the gore line using flexible conductive epoxy. Mesh/rib tooling marks

LMSC-D714613

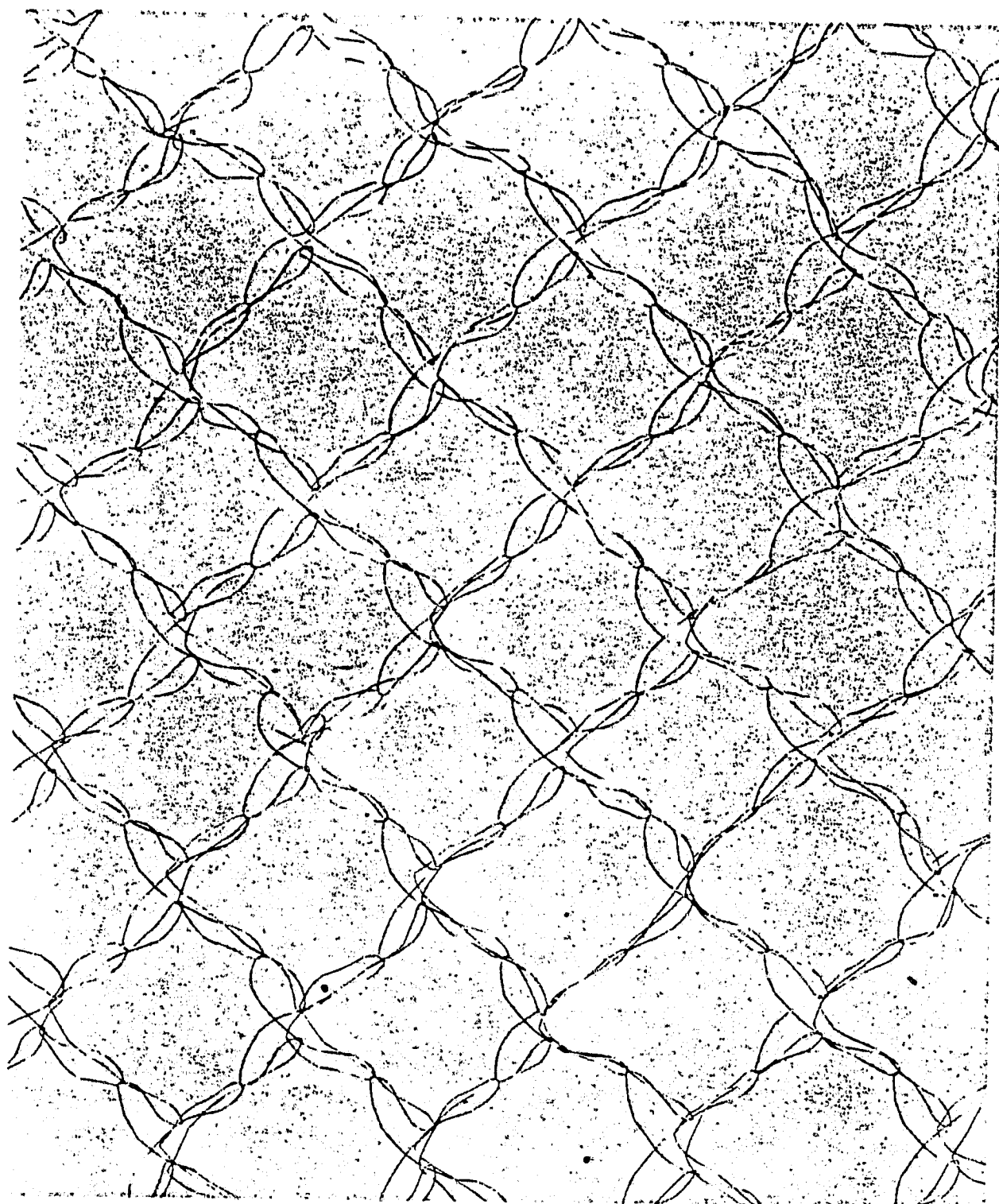


Figure 11. Moly/Gold Knit Mesh

are attached to the mesh. The mesh is cut, rolled, and delivered to the reflector assembly area where the panels are indexed to the pre-marked rib hub assembly and sewn in place.

#### 2.1.2.3 Hub

The reflector hub is shown in drawing DDS-140 Figure 12 and Figure 13. This hub is constructed from two machined 7075-T6 aluminum forgings tied together with 0.024 inch 7075-T6 aluminum conical shear panels and stiffened with machined ZK60 magnesium I-beam sections. The inner machined ring becomes the spacecraft interface plane while the outer ring provides attachment for the rib hinges. The top and bottom hub covers are comprised of 0.014 AZ31B magnesium sheet material as a non-structural element, and machined ZK60 magnesium I-Beam sections that interface with the hub stiffeners via four number 10 titanium bolts. These sections provide the structural load path in the axial direction for the stowed rib mass during ascent. The view to space of the stowed rib and mesh pack is occluded by the use of aluminized Kapton thermal radiation shields.

The main structural elements are thermally protected by a multi-layer radiation blanket. This blanket is comprised of a one mil outer layer of aluminized Kapton (Kapton out) and 1/4 mil doubly aluminized mylar radiation layers interleaved with lightweight polyester knit. The blanket is attached to the top and bottom of the hub covers with hook and pile fasteners. Local grounding tabs or straps are provided that penetrate the blanket at selected positions and mechanically attached to the hub structure.

The overall assembled hub configuration is designed to provide a high torroid bending stiffness. This design goal was established from the exacting contour accuracies required. It was found on the ATS-6 program that it was desirable to minimize the hub rotation induced rib

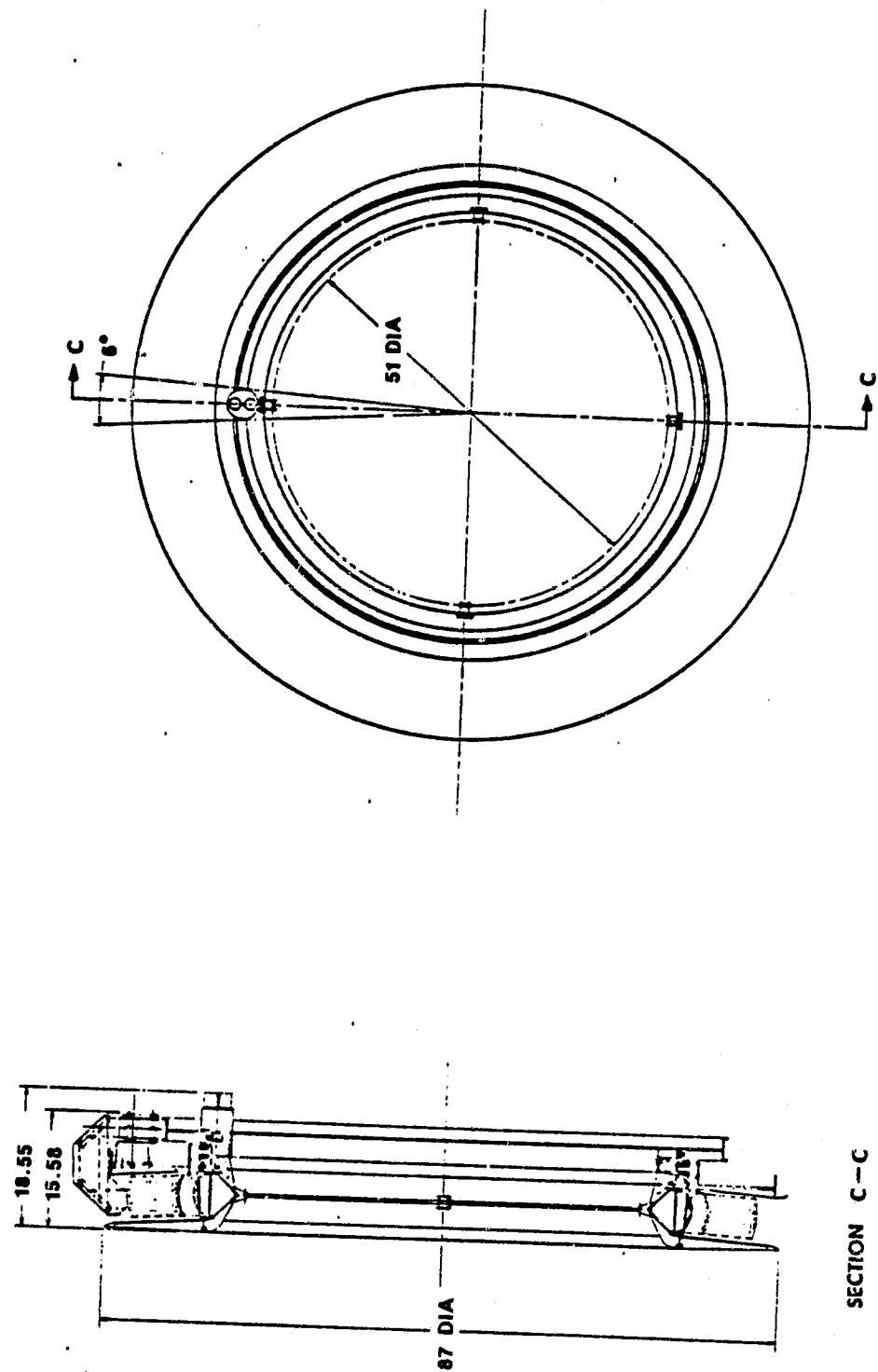


Figure 12. Stowed Configuration

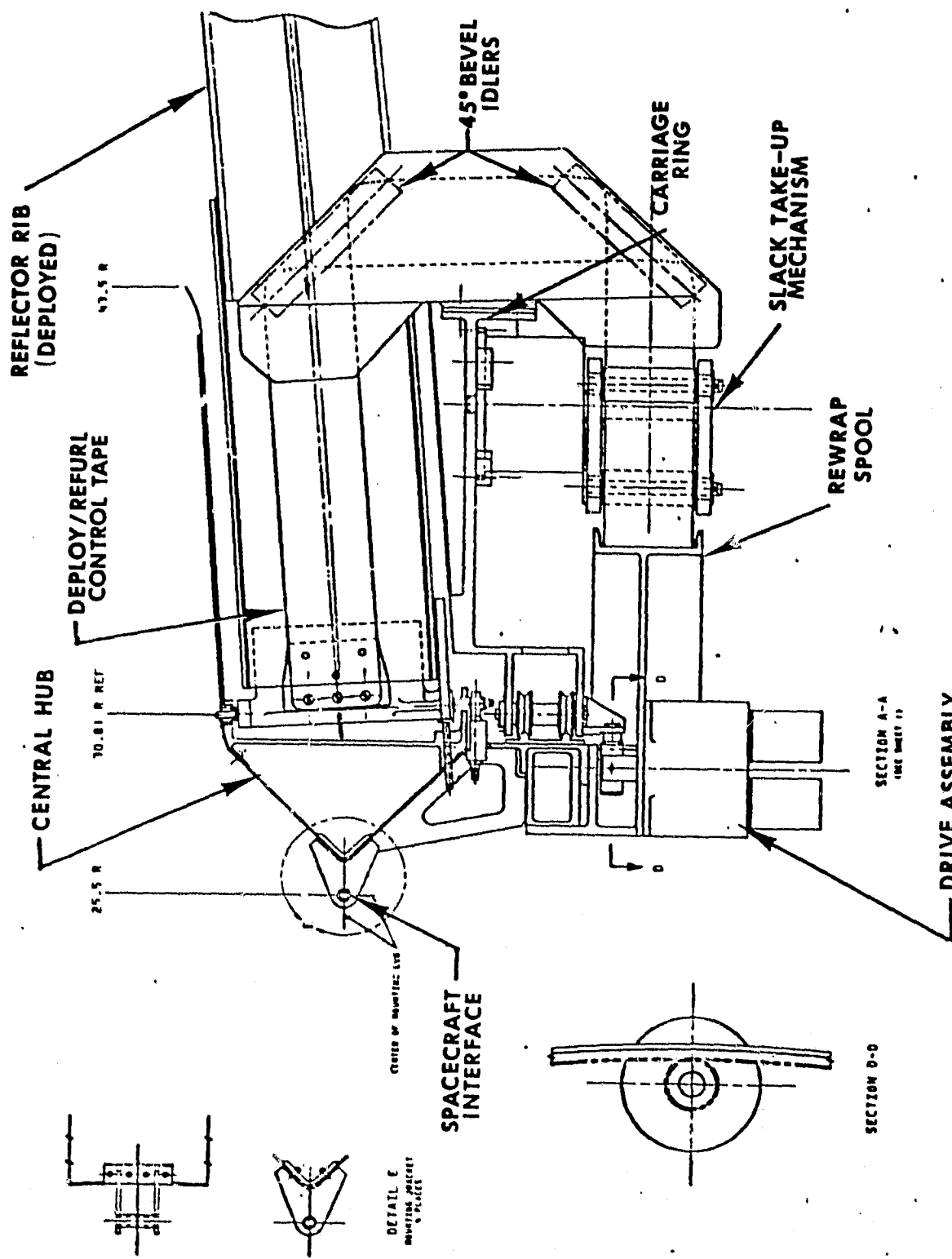


Figure 13. Hub Section And Drive System

deflections during contour setting and subsequent measurements.

Contour adjustments is provided by a differential pitch lead screw mechanism as in Figure 14. This device consists of a concentric right hand threaded shaft and barrel. The internal thresh is a 32 pitch 1/4 inch diameter while the barrel outside thread is a 28 pitch, 3/8 inch diameter. One revolution of the barrel causes the internal shaft to advance 0.0045 inches and produces a proportional rib tip motion. This system provides high precision contour adjustment sensitivity.

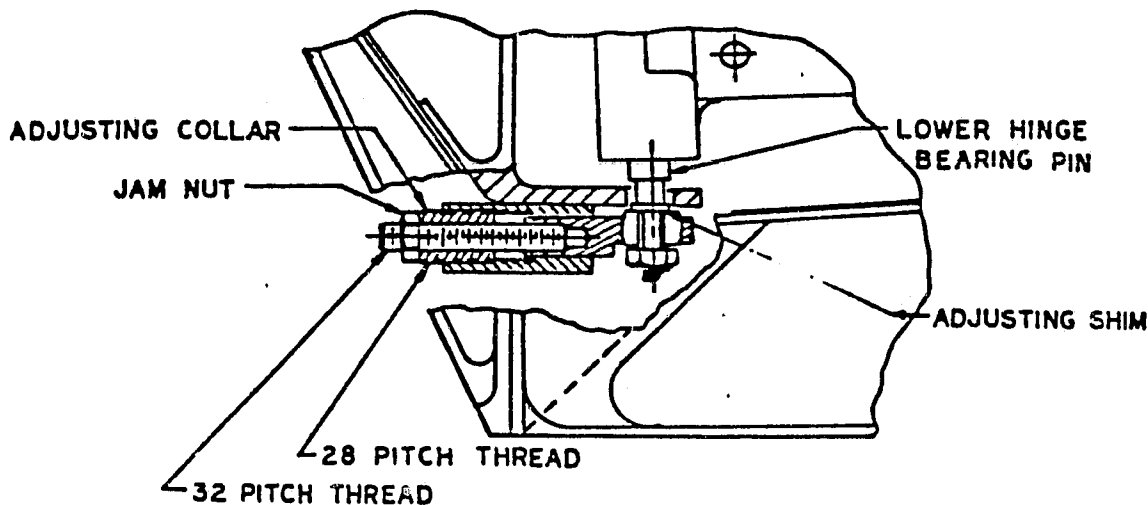


Figure 14. Rib Adjustment Mechanism

#### 2.1.2.4 Deployment Control Device

The deployment control mechanism, called the "re-wrap" concept is essentially a reel-to-reel tape drive. With the reflector in the stowed configuration, a restraint tape is attached at the central hub and wrapped circumferentially along every third rib. This tape then travels over a set of 45° bevel idlers, through a slack take-up mechanism and terminates at

a spool that is a part of the central hub (ref. Figure 13). The bevel idlers are mounted to a gear driver carriage ring mounted on bearings. In operation, the drive motor is energized driving the carriage ring. This causes the tape to travel over the bevel idlers, and re-wrap around the central spool. This gradually releases the radial pressure on the stowed ribs, allowing the self contained stored energy to deploy the ribs at a controlled rate. For stowage, the operation is simply reversed causing the ribs to again wrap around the central hub.

#### 2.1.3 Feed Support Structure

Previous programs have devoted little attention to definition of the feed support structures required to support a deployable antenna design. As a result a review was conducted of the candidate design approaches and the significant characteristics of each design developed. This review is overviewed in Figure 15. These results indicated that the most probable design concept in terms of weight efficiency and stability should rely on a triangular geometry.

Two of the designs, the Astromast and the Tri-Extender have been developed to the point of concept demonstration. The Astromast has been well characterized and demonstrated to be capable of automatic extension and retraction. The Tri-Extender as previously configured showed potential for increased stiffness due to a different design mechanism but had only been developed as a one way deployable system. As a result, the study activity was directed at investigating a modification and characterization of the Tri-Extender to provide an alternate approach to the Astromast. It was felt that a design approach selection could be made in a future study and the mast limitations on antenna technology growth indicated would be similar with either system.

The key elements in the LMSC Redeployable Mast are the three lenticular shaped longitudinal members which can support an appreciable longitudinal

## FEED SUPPORT STRUCTURES SURVEYED

Figure 15

## FEED SUPPORT STRUCTURES SURVEYED

load when erect, but which can be folded upon themselves through the application of lateral and axial forces, as shown in Figure 16.

Figure 17 illustrates the way in which the characteristics of the lenticular members are used to obtain a lightweight mast design. The deployed section lengths and the dimension "b" between the lenticular members are bounded by several considerations including optimum column lengths between hinges, stowage diameter limitations, minimum batten and hinge weights, etc. The previous study showed that, within reasonable limits, aspect ratios of 0.5 to 1.5 are compatible with stowage constraints and a value of 1.0 provided the optimum stiffness/weight results. For resisting torsional and lateral shear forces, wire tension cables are provided. The battens are necessary for supporting section hinges and for resisting the lateral, destabilizing cable reactions.

Figure 3 shows the overall mast system and emphasizes the stowage and deployment systems. The inner system performs the actual, section-by-section deployment and retraction of the mast through the use of three synchronous motor, sprocket, chain and deployment cog systems. It also serves as the bottom mast section until that section, itself, is fully erect. The guide rails in which these devices operate, are also provided with ramp cams which actuate the strikers for collapsing the lenticulars during retraction. The outer base system acts as the stowage bay for both the mast sections and the inner base system which must be extended during mast extension or retraction, but is retracted into the outer base system during full stowage. A chain drive system is also provided for the latter purpose. In detail, the operating sequences for deployment and retraction are as follows:

1. Extend the upper portion of the extension/retraction cage.  
This is accomplished with a chain drive system.
2. Deploy the boom by activating the deployment/retraction chain drive. This drive is a chain loop at each of the three corners of the mast. Three cogs are attached in such a manner that

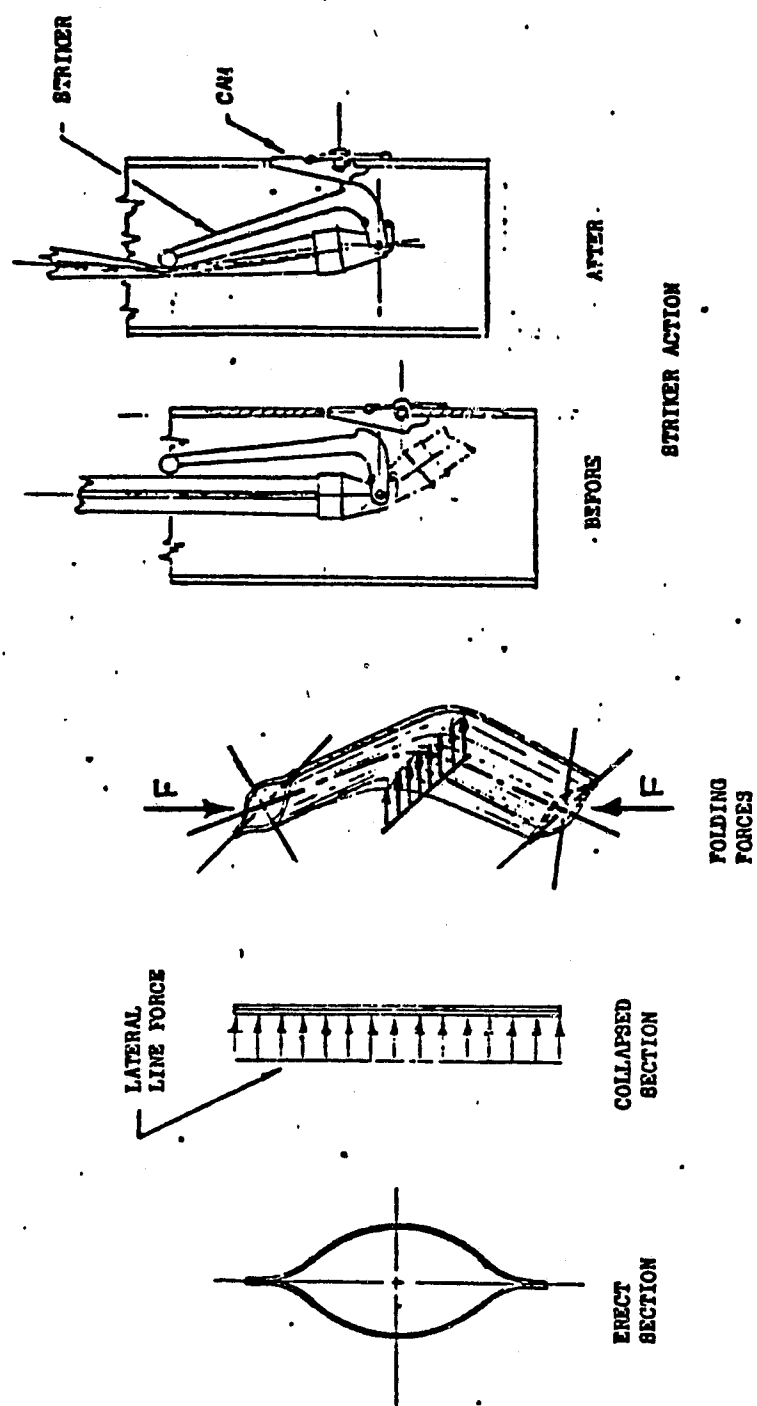


Figure 16. Mast Collapsing Member

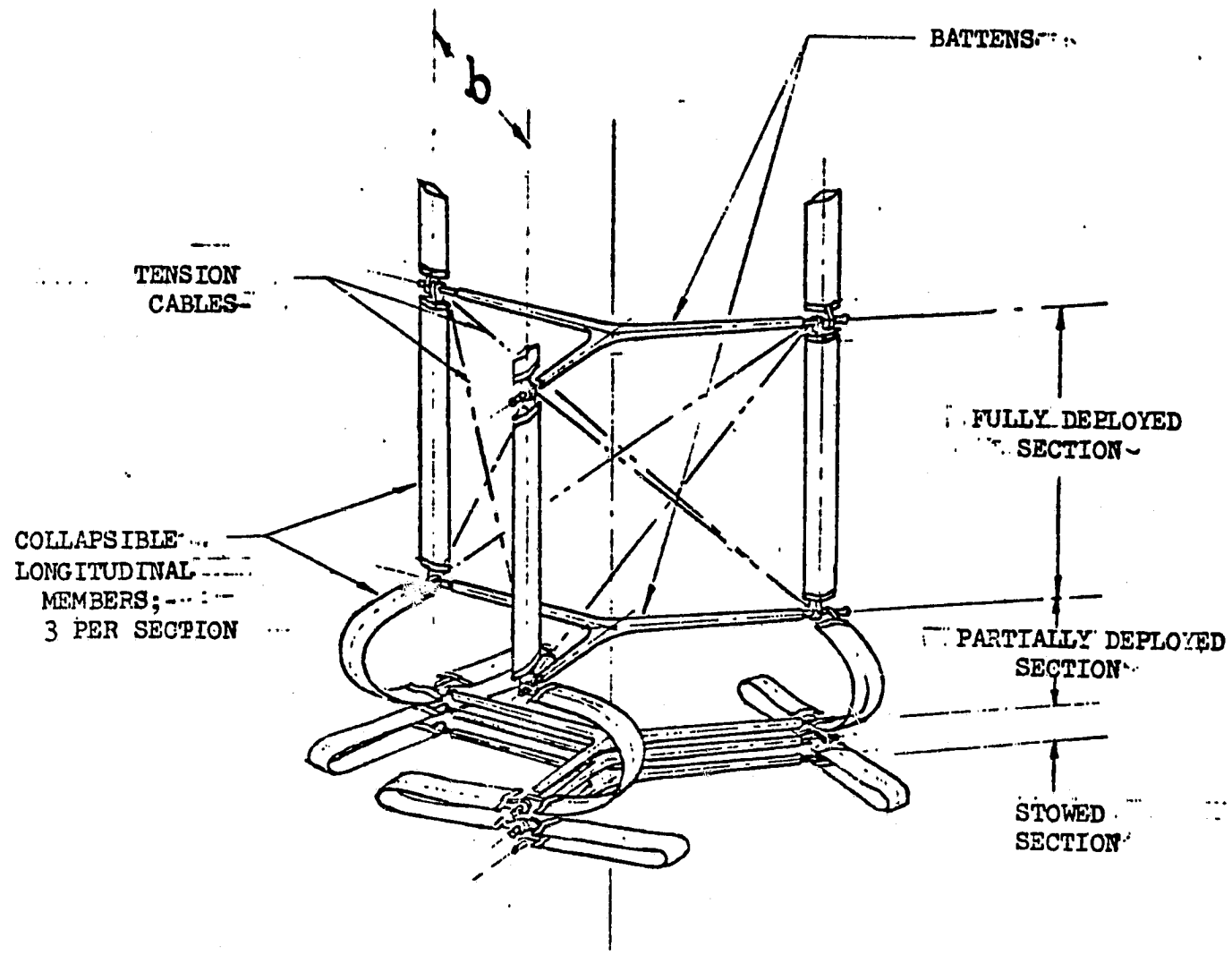


Figure 17. Mast Section Stowing Sequence

cog to cog linear dimension matches the linear dimension of one mast section. One cog engages the compression spider (batten) at the top of the stowed stack while the other releases the batten at the top of the just deployed section. During the deployment of each section, the cog follows the batten through the section extension, thereby retaining the stored energy of each section within the extension system. This follows until all of the sections have been erected. The incrementally deployed mast is stabilized at all times during deployment because the portion deployed is fastened at three points to the moving cog chains.

3. Retract the boom by reversing the direction of the deployment/retraction chain drive. This works identically to the deployment sequence but in reverse. The additional requirement is that the longerons be buckled laterally as the cog is engaged and then apply a compressive axial load to complete the fold stowing of the lenticular section longerons. A trip arm built into the longeron end accomplishes this lateral buckling. The longeron first engages a one way ramp on the side of the chain carrier. The loading caused by the ramp causes a local lateral load on the longeron which collapses the lenticular cross section. Cog retraction folds the longeron. Alternating the placement of the trip arm, or striker, on the longerons allows folding in alternate directions to minimize stowed height.
4. Retract the upper portion of the extension/retraction cage. The cable deployment system is reversed.

#### 2.1.4 System Ascent and Deployment

The configuration is reasonably well defined for maximum efficiency of an offset fed antenna system. Figure 18 presents an overview of the ascent sequence through the operational state of the vehicle. The STS stack shows an IUS attached to a vehicle from which the stowed feed support tower and reflector are attached. After achieving the desired operational orbit the deployment sequence begins with the tower extending, separating the vehicle from the reflector. The final event is the reflector deployment which occurs after the feed support tower has been completely deployed. The operational vehicle configuration was chosen to place the feeds, electronics and electrical power system components together for maximum efficiency since for the offset configuration this package does not block the antenna aperture.

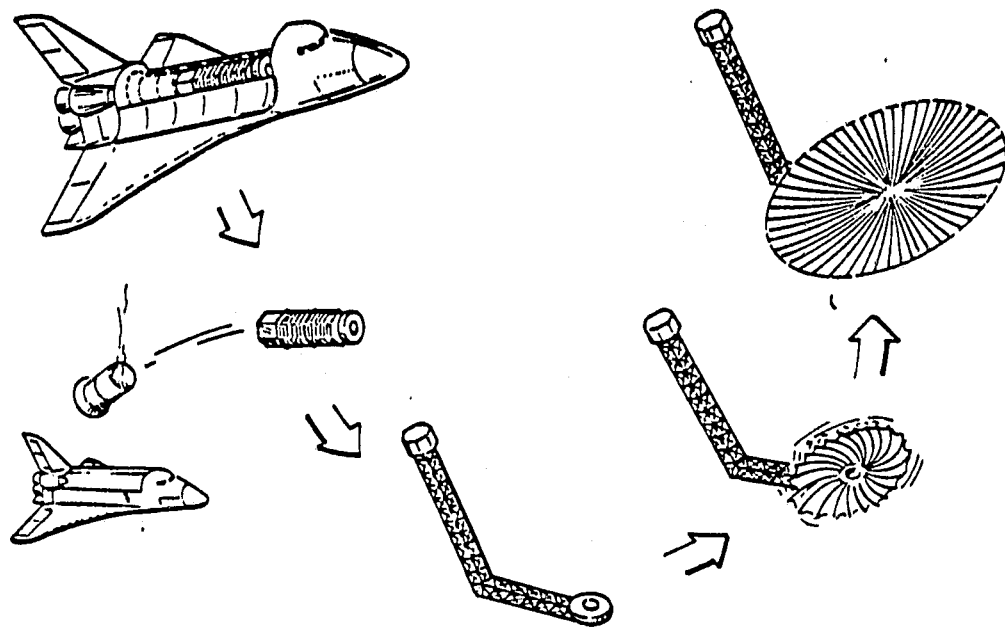


Figure 18. Offset Fed Antenna System Operational Sequence

The symmetric antenna system can be used in a similar configuration. The system performance would be greatly degraded, however, by the blockage of the aperture from the feed support tower (ref. Figure 1) and by the solar arrays which would be attached to the feed located in the equipment section. An alternate configuration would be to locate the solar arrays aft of the reflector and accept the shadowing of the solar arrays by the reflector structure.

## 2.2 PERFORMANCE MODEL

### Study Approach

The approach taken to develop the parametric design and performance data focussed on the construction of computer aided reflector and mast design packages. The reflector design package was constructed to accept basic material and structural element characteristics and develop design solutions which satisfied these inputs and the mission constraints of weight, stowed diameter and antenna system geometry. The developed designs were then analyzed to determine the extent of orbital and assembly surface errors, deployment integrity, and development costs.

Having defined the reflector size and operational frequency, a mast design could be developed with a design constraint that the pointing error be held to less than 0.05 beamwidths. The mast design package approach was similar to the reflector package.

This developed program is overviewed in Figure 19.

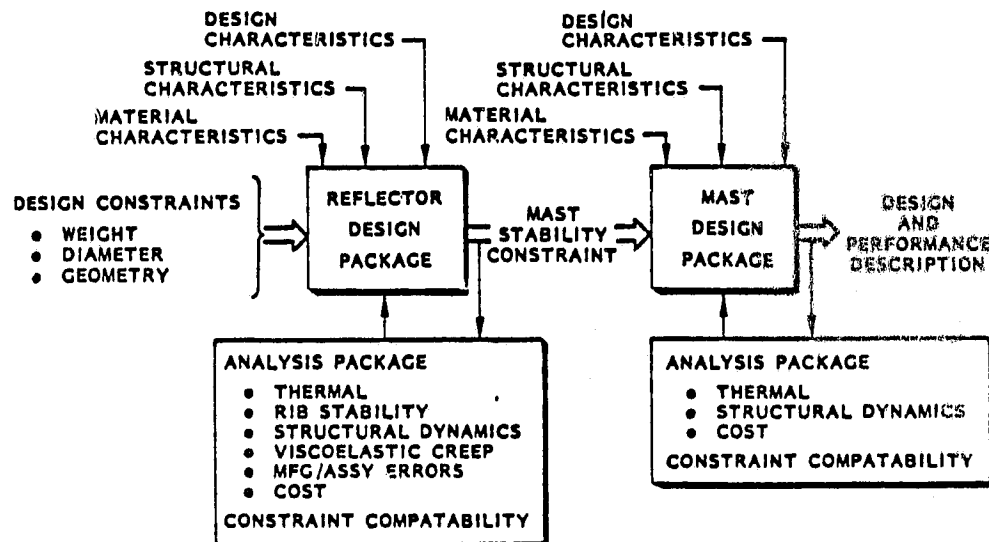
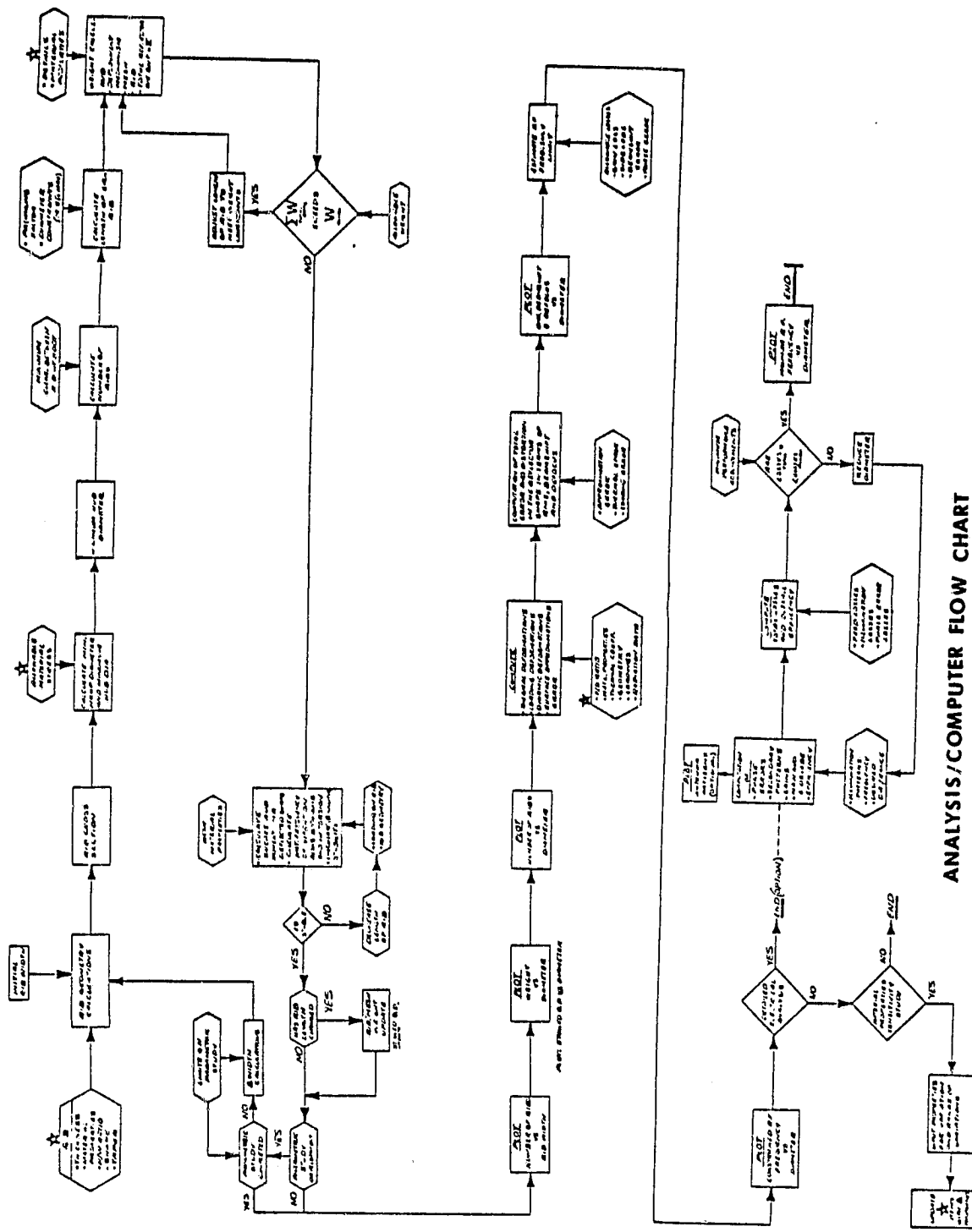


Figure 19. Modeling Approach

The computer program assembled for this study of necessity provided more capability than a simple parametric study tool. In fact, it is required to generate a complete preliminary design and performance analysis. The flow chart for the program is presented in Figure 20. An overview of this flow chart is presented in Figure 21 and was selected to introduce the operation.

Figure 21 was developed from study case input data, computer programs, and output data. There are thirty six input values, two of which describe mission constraints (weight and stowed diameter). The remaining variables are design and material characteristics. The main computer program develops the requirement compatible antenna designs and directly outputs a summary of the key output parameters while writing all of the detailed information to a file. Any or all of the design cases can be recovered in a readable form at a time selected by the user. This detailed information contains complete element design descriptions, weight breakdown and performance budget and can be used as a baseline preliminary design.



## ANALYSIS/COMPUTER FLOW CHART

## DETAILED DESIGNS

卷之三

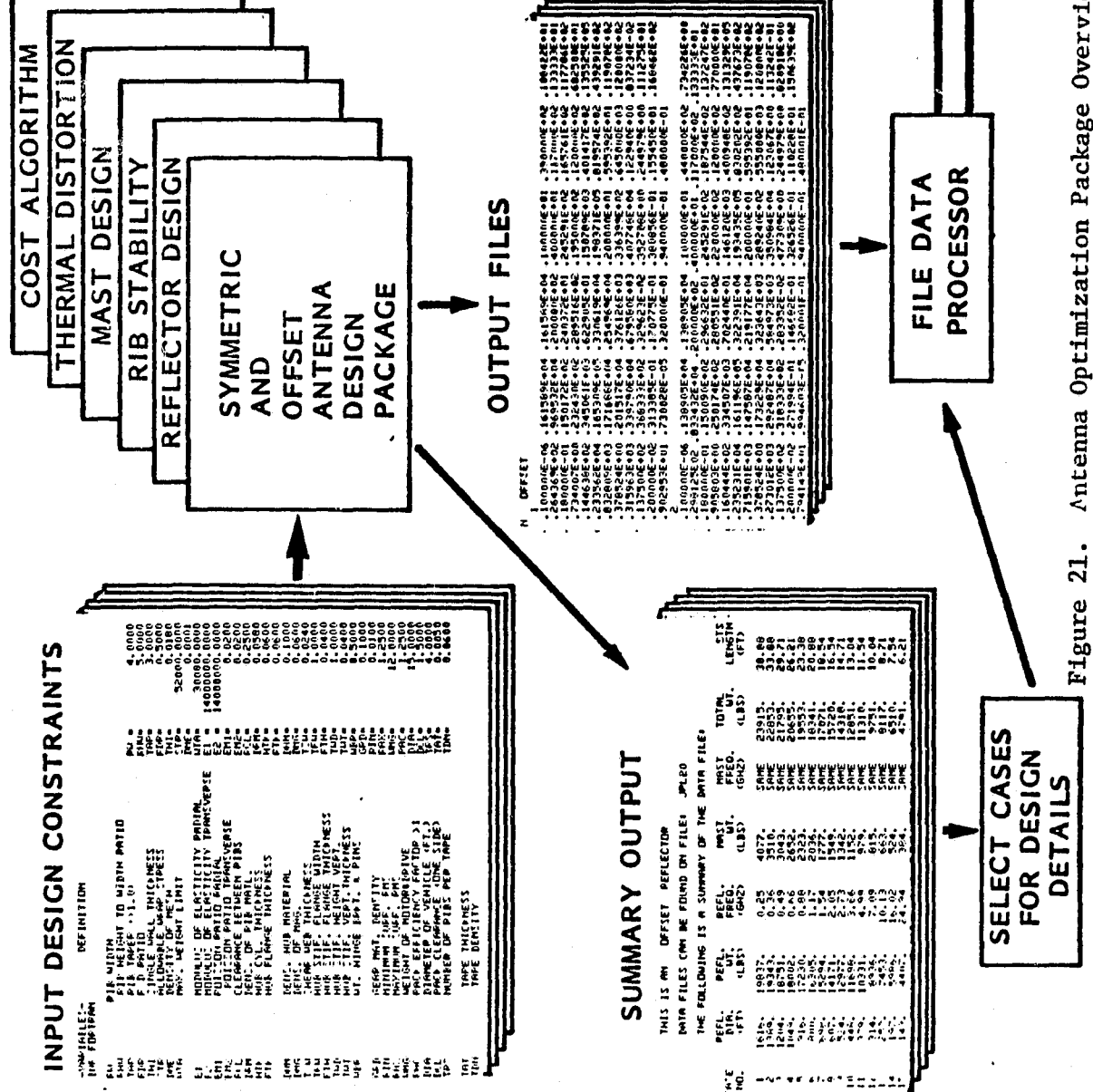


Figure 21. Antenna Optimization Package Overview

### 2.2.1 Design Package Computer Program

The reflector design program (see Appendix A) reads a data file which contains all of the design inputs and constraint information. These parameters, examples of which are shown in Figure 22, can be changed at the time of program execution.

The first calculation performed is that of the minimum wrap radius for the predetermined rib geometry. The relationship used is

$$\sigma = \frac{E t}{2(1-\mu_{1-2} \mu_{2-1})} \left[ \frac{1}{R_1} + \frac{\mu_{1-2}}{R_2} \right]$$

where

- E = Youngs Modulus
- t = Material Thickness
- $\mu_{1-2}, \mu_{2-1}$  = Poisson Ratios for each axis
- $R_1$  &  $R_2$  = Respective Flattening and Wrapping Radii
- $\sigma$  = Combined Flattening and Wrapping Stress.

The flattening radius R is determined from the height (h) and width (w) of the rib according to the relationship

$$R = \frac{1}{8w} (w^2 + h^2)$$

The design input file contains the rib root geometries to determine this along with a linear taper ratio to determine the width of the rib at the tip. The lenticular radius determined for the root section is used in conjunction with the width to determine the rib tip cross section height.

-PUN SINGH

REFLECTOR GEOMETRY GROWTH PROGRAM

NEED HELP(Y OR N)? N

PRESET FILE NAME(AS)? JPLIN

PRINT PRESET(Y OR N)? Y

```

RW= 1.0000
RHW= 4.0000
THP= 3.0000
FDR= 0.5000
THI= 0.0190
STR= 52000.0000
DME= 0.0001
MTA= 30000.0000
E1= 14000000.0000
E2= 14000000.0000
EM1= 0.0200
EM2= 0.0200
POL= 0.2500
DRM= 0.0590
HTK= 0.0600
FTK= 0.0500
DHS= 0.1000
IMG= 0.0500
TSW= 0.0240
TFW= 1.0000
FTH= 0.0400
TWD= 1.0000
TNT= 0.0400
MBR= 0.5000
GRD= 0.1000
RIN= 0.0100
PAK= 1.2500
WMS= 12.0000
PHC= 1.2500
DIA= 15.0000
DCL= 1.5000
TRS= 4.0000
TAT= 0.0050
TDN= 0.0500

```

-----

READY FOR INPUT DATA

```

RW
=4.
RHW
=5.
FDR
=2.
NOW

```

```

DATA OUTPUT FILE NAME =
TR1

```

```

OFFSET(1) OR SYMMETRIC(2) ? =
1

```

THIS IS AN OFFSET REFLECTOR

DATA FILES CAN BE FOUND ON FILE: TR1

THE FOLLOWING IS A SUMMARY OF THE DATA FILE:

CASE NO.	LEFL. (FT)	REFL. (IN.)	REFL. (LBS)	MAST (FT)	MAST (LBS)	FREQ. (GHZ)	FREQ. (LBS)	TOTAL (LBS)	STS LENGTH (FT)
1	2356.	25567.	0.16	36512.	0.12	52079.	555.04		
2	1974.	25389.	0.24	30459.	0.17	55856.	547.04		
3	1677.	24954.	0.33	25979.	0.23	50733.	455.04		
4	1441.	24157.	0.45	22254.	0.31	46411.	400.39		
5	1219.	23213.	0.51	19290.	0.42	42503.	347.39		
6	1059.	22203.	0.50	16303.	0.55	39011.	303.04		
7	950.	20979.	1.06	14593.	0.72	35652.	265.04		
8	830.	19409.	1.39	12935.	0.94	32244.	232.04		
9	724.	17959.	1.33	11199.	1.24	29157.	202.71		
10	630.	16322.	2.44	9739.	1.54	25050.	175.71		
11	544.	14742.	3.28	8414.	2.20	23156.	153.04		
12	455.	12963.	4.49	7203.	3.01	20165.	131.39		
13	393.	11237.	5.32	6095.	4.22	17323.	111.39		

ORIGINAL PAGE IS  
OF POOR QUALITY

Figure 22. Example Of Summary Output

At this point the maximum number of ribs (N) that can be physically placed around the determined minimum hub of radius  $r$  is calculated from

$$N = \frac{\pi}{\sin^{-1} \frac{(w+c)}{2r}}$$

where

w = Rib Width

c = Rib to Rib Spacing

Having determined the number of ribs, their maximum length, and therefore the reflector diameter can be determined by using the available annular area (a) between the hub ( $r_h$ ) and the STS envelope( $r_s$ ).

$$A = \pi (r_s^2 - r_h^2)$$

But A is also equal to the projected area of the stowed rib package or

$$A = \frac{N L t}{\eta}$$

where

L = The Rib Length

$\eta$  = Packaging Efficiency

N = Number of Ribs

so that  $L = \frac{\eta \pi}{N t} (r_s^2 - r_h^2)$ .

Having determined the maximum aperture diameter with a minimum number of ribs the surface approximation error is calculated and is compared to a predetermined maximum RMS. The number of ribs is incremented by four until the calculated RMS error is less than the desired maximum. At this point, the program computes the hub weight based on the geometry described in Section 2.1.2.3, the rib weight, and the mesh weight

which is optimized to the maximum operating wavelength of 30 times the current RMS error ( $30 \delta$ ). The thermal distortion, manufacturing and viscoelastic creep errors are calculated. These errors are combined through an RSS and the maximum operating frequency is determined from the  $30 \delta$  relationship. The stowed mast geometry is defined based on the allowable STS diameter envelope the desired f/D ratio and the allowable beam shift. Thus defined, the mast weight structural and thermal properties are determined.

At this point the program calls a costing subroutine to determine the projected development and production costs of the reflector and feed support structure. This cost algorithm is based on the ATS-6 program performance and on historical data points on several quoting exercises for other programs. It utilizes the frequency, diameter, and f/D ratio with empirically derived exponential factors. These factors are then applied to a normal program percentage breakout of design, analysis, test, manufacturing, and materials.

These data are written to a data file with identification marks and also to the computer terminal in summary form.

The next constraint the program recognizes is the predetermined minimum RMS for the reflector.

If the program finds no cases that satisfy the maximum RMS condition with the minimum hub size, the hub diameter is incremented to a larger value thereby allowing more ribs and a corresponding smaller aperture and the process is iterated until at the limit the hub and the STS envelope are the same size indicating a solid non deployable reflector is required.

At this point, a second program is exercised to display the particular parameters of a given reflector. Figure 22 contains an example of the sum-

mary output results while Figure 23 illustrates the detail "PRINT" program output.

### 2.2.2 Analytical Description of an Off-Set Wrap-Rib Reflector

A computer program has been prepared in Fortran IV which describes the off-set wrap-rib reflector. The program optimizes the location of each rib by systematic search, and computes the optimum location for that rib. The program contains a generalized illumination function which can be executed. If an illumination function weighting is not desired, the RMS value for uniform illumination can be obtained. Although the program was developed for an offset reflector, it applies to symmetric reflectors also by setting the off-set dimension equal to zero.

The program provides for up to 20 subintervals in the radial direction. The program operates by iterating on the focal length of the rib to arrive at the minimum RMS for the reflector.

The analytical derivation for this solution, a listing of the program symbols, and a sample run are contained in Appendix F.

### 2.2.3 Thermal Distortion Analysis

This part of study focussed on obtaining an estimate of the surface distortion of large wrap-rib parabolic reflectors with lenticular rib section in an outer space environment.

A computational scheme is developed which considers the effects of thermal and mesh pretension loads simultaneously. For a given orbit and its orientation, the thermal program given the temperature gradient along the length and the height of a lenticular rib section. The

TYPE NAME =  
TRI  
CASE NO. =  
13  
.....

THIS IS AN OFFSET REFLECTOR

DATA FILE: TRI CASE NUMBER: 13

DESCRIPTIVE DATA FOR REFLECTOR DESIGN:

REFLECTOR FOCAL LENGTH (FT.) =	645.40
SECTION DIAMETER (FT.) =	323.20
FOCAL LENGTH TO DIAMETER RATIO =	2.00
NUMBER OF RIBS =	94.00
SURFACE APPROX. ERROR (IN. RMS) =	0.0193
PIR HINGE RADIUS (IN.) =	63.51
PIR TIP RADIUS (IN.) =	1939.20
PIR FOOT HEIGHT (IN.) =	20.00
PIR FOOT WIDTH (IN.) =	4.00
PIR TIP HEIGHT (IN.) =	11.70
PIR TIP WIDTH (IN.) =	1.33
PIR THICKNESS (IN.) =	0.0190
HUB OUTSIDE DIAMETER (FT.) =	14.87
HUB INSIDE DIAMETER (FT.) =	9.50
HUB HEIGHT (IN.) =	24.53

WEIGHT SUMMARY:

HUB RING =	40.56
SHEAR WEB =	33.21
CHEAR WEB RING =	2.63
HUB STIFFENERS =	27.42
HUB SP. INS =	13.15
HINGE ASSEMBLY =	47.00
MOTOR & GEAR DRIVE =	12.00
TAPE GUIDES =	16.45
TAPE PEAL ASS'Y =	31.97
DEPLOY/RETRACT TAPE =	159.34
RINGS GEAR =	14.99
DRIVE SUPPORT BKT =	69.49
HOLE COVER =	39.32
RIBS =	6155.73
MESH =	1199.55
 TOTAL WEIGHT =	7771.33
CONTINGENCY (20%) =	1554.27
 MAXIMUM WEIGHT =	9325.60 POUNDS

ESTIMATED COST DATA:

ESTIMATED DEVELOPMENT COST (MILLIONS) =	177.46
ESTIMATED RECURRING COST (MILLIONS) =	87.75

THIS IS A TRI-EXTENDER MAST CONFIGURED FOR  
THE REFLECTOR FOUND IN:

DATA FILE: TRI CASE NUMBER: 13

DESCRIPTIVE DATA FOR DESIGN:

MAST LENGTH (FT) =	919.35
OFFSET LENGTH (FT) =	162.96
PARALLEL LENGTH (FT) =	556.50
WIDTH (FT) =	9.93
Bay LENGTH (FT) =	9.23
ASPECT RATIO =	1.04
STOWED DIAMETER (FT) =	13.75
STOWED LENGTH (FT) =	30.57
NATURAL FREQUENCY (CPS) =	0.0911
THERMAL BEAM SHIFT (DEG) =	0.0007
FREQ. FOR 0.0589 (GHZ) =	9.51

WEIGHT SUMMARY:

LONGERON =	1279.79
BATTENS =	230.93
CABLES =	13.27
JOINTS =	257.00
MOTOR DRIVE =	12.00
SUPPORT STRUCTURE =	109.32
 TOTAL WEIGHT =	1911.30
CONTINGENCY (20%) =	392.26
 MAXIMUM WEIGHT =	2293.56 LBS.

WEIGHT PER DEPLOYED INCH = 0.2223

MAST DEVELOPMENT COST (\$M) = 43.65  
MAST RECURRING COST (\$M) = 21.59

THIS IS AN OFFSET REFLECTOR

DATA FILE: TRI CASE NUMBER: 13

THE FOLLOWING IS A REFLECTOR LOSS BUDGET:

SURFACE APPROXIMATION =	0.0193
THERMAL ERROR =	0.0404
PIR CONTOUR ERROR =	0.0020
PIR SEGMENT JOINT ERROR =	0.0075
PIR ROOT TO TIP INST. ERROR =	0.0033
PIR VISCOELASTIC "CREEP" ERROR =	0.0032
 TOTAL SURFACE ERROR =	0.0457 INCHES RMS

TAPE NAME =  
END

EXIT

Figure 23. Example Of Detail Output

effects of the thermal load and mesh pretension are used to calculate the rib distortion and the resulting degradation of the reflector surface integrity.

The thermal effect is iteratively combined with the initial mesh pre-load to arrive at the final distorted shape of the rib from which surface RMS relative to a perfect paraboloid is calculated.

The temperature routine contained in Appendix B was based on a steady state 14 transverse node model developed at LMSC in 1977 and contained in Appendix C. It has been enhanced for this project to include the effects of solar angle changes, the addition of multilayer blankets, and as illustrated in Figure 24 the rib-to-rib shadow effects as a function of the number of ribs, the solar angle, the f/D ratio, and the radial position along the rib. For conservatism it considers only the ribs which would be normal to the sun vector (at a solar angle of 0°). Appendix B also contains the distortion routine.

Appendix D gives a brief description of the analytical procedure used to develop the distortion model. Appendix E describes the analytics required to describe the rib cross sectional properties.

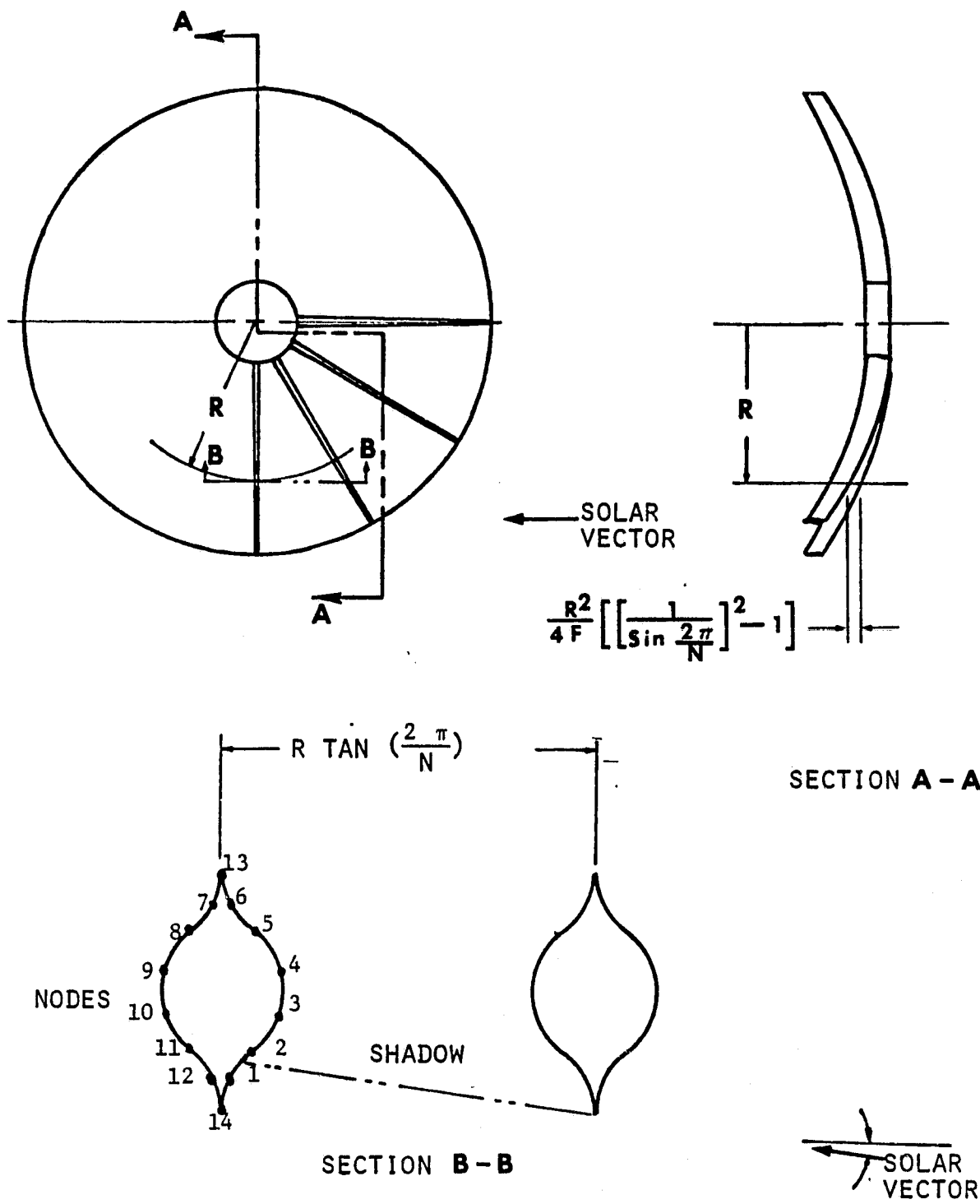


Figure 24. Thermal Model Geometry

## 2.3 PERFORMANCE PROJECTIONS

This section of the report is devoted to presentation of the data developed during the study on the performance projections of the symmetric and offset wrap-rib antenna designs. The most significant of the results is of course the projection of the upper bound of surface quality as a function of diameter. These data are presented in Figure 25. The limit on frequency of operation was defined as a total RMS error allowable of 1/30 of the operating wavelength. The RMS was an area weighted function only, i.e., a uniform illumination case. Errors included were surface approximation, thermal distortion, rib contour manufacturing, rib assembly, reflector assembly and graphite epoxy viscoelastic creep. It is interesting to note that constraints on achievable operating frequency were reflector design induced for diameters less than 95 m and STS diameter for apertures above 95 m.

### 2.3.1 Weight Impact on Aperture Size

The aperture limit derivation was performed with a weight constraint of 3620 Kg, a full STS load. These data have been expanded for the larger diameter region and displayed for both offset and symmetric geometries in Figure 26.

Two other cases were considered. The first was a limit of 2270 Kg which is compatible with a synchronous component for assembly at altitude. The 681 Kg case represents a subsystem weight compatible with a full spacecraft system to be delivered to synchronous orbit.

The performance advantage of the offset geometry is evident in the figure. Two effects contribute, those being the effective doubling of the focal length due to the geometry and the improved approximation error due to an integral reduction in surface curvature. The result being a higher operating frequency for the same diameter for an offset reflector.

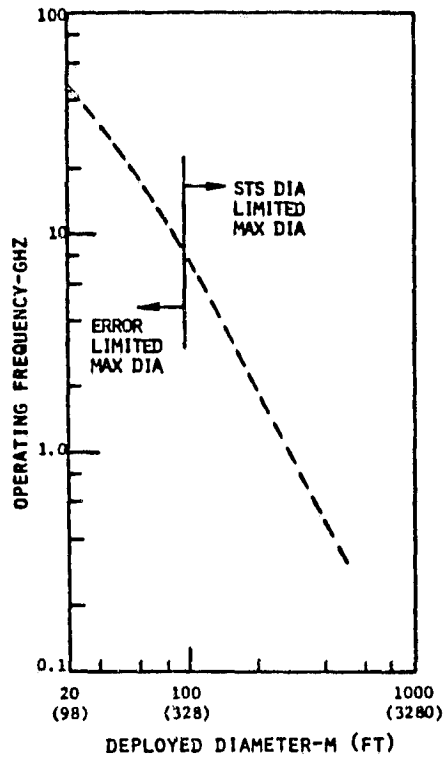


Figure 25. Upper Limit of Surface Quality

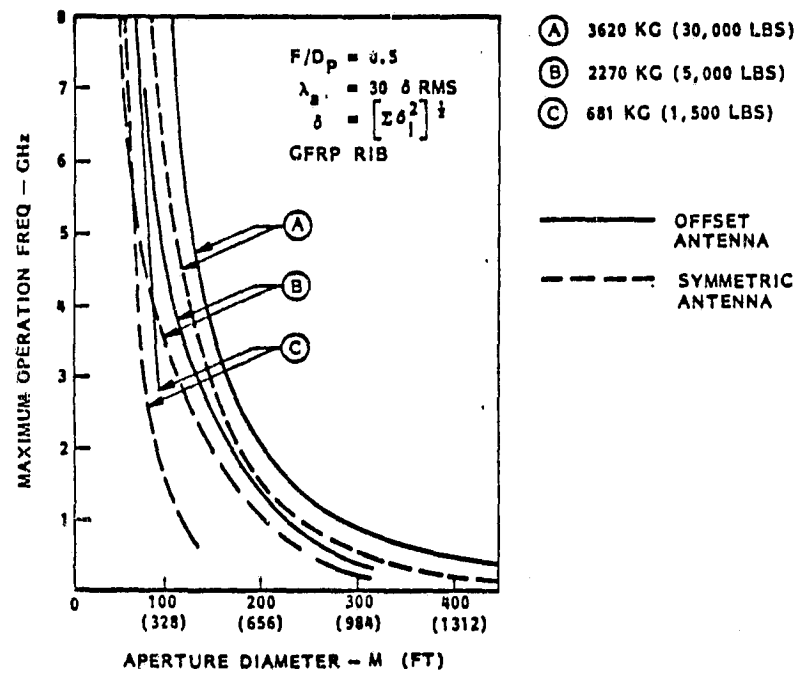


Figure 26. Weight Constrained Aperture Limits

### 2.3.2 STS Stowed Volume

The algorithm constrained the developed parametric designs so that the stowed diameter of the reflector and feed support tower never exceeded the 4.57 m limit of the STS bay. Figure 27 displays the stowed package length for the reflector and feed support tower stack. The results indicate there is no significant STS volume constraint imposed on the growth of the concept. The length allocation for a complete load is approximately 17 m.

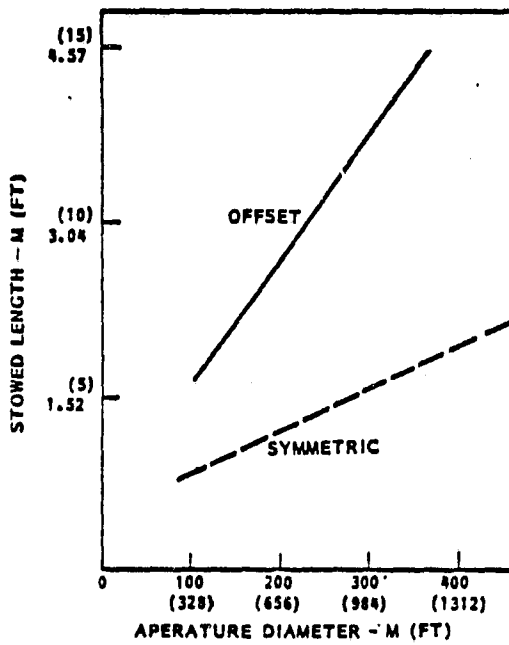


Figure 27. Antenna Systems Stowed Length Requirements

### 2.3.3 Surface Figure Considerations

The surface figure of a graphite epoxy reflector structure is a function of six separate contributors; rib segment fabrication, rib assembly, reflector assembly, viscoelastic creep, thermal distortion, and designed surface approximation. The total effect of these errors was calculated as the root-sum-squared (RSS) of the individual error components.

The surface approximation and the thermal distortion are the dominant error contributors for the cases performed. It is interesting to note from Figure 28, that for the smaller (less than 300 meters) symmetric apertures and correspondingly higher frequencies, the thermal distortion is the larger of the two while at larger apertures and lower frequencies, the surface approximation dominates. This is due to the rib limiting effect of the STS diameter constraint which takes over at about that point.

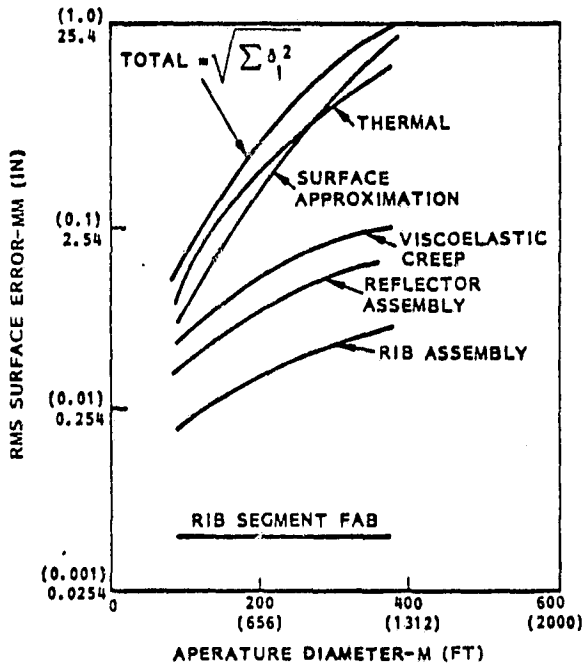


Figure 28. Surface Figure of STS Diameter Constrained Symmetric Antenna

The longer f/D ratio for the offset antenna causes the surface approximation errors to be less than for the symmetric system. As a result, the thermal distortion error for the offset reflector, Figure 29, is the dominant factor throughout the area of interest.

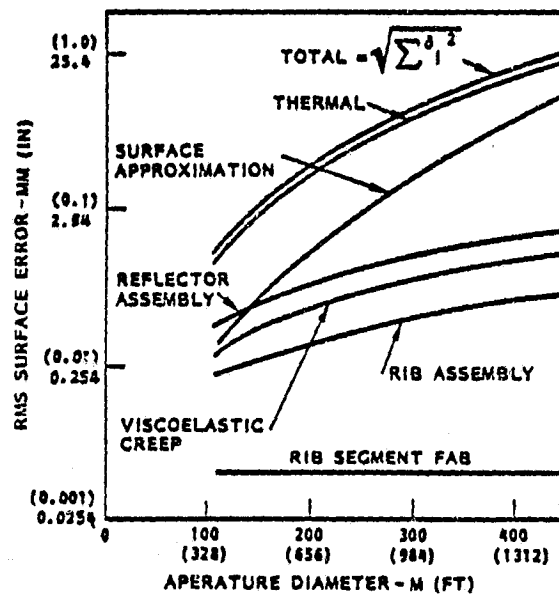


Figure 29. Surface Figure of STS Diameter Constrained Offset Antenna

When the weight limit of 2300 Kg was applied, the surface approximation error for the symmetric case was found to become dominant at a much smaller aperture. This occurs due to the decrease in the number of ribs that must occur at a given diameter in order to meet the weight constraint. This effect can be seen by comparing Figures 28 and 30.

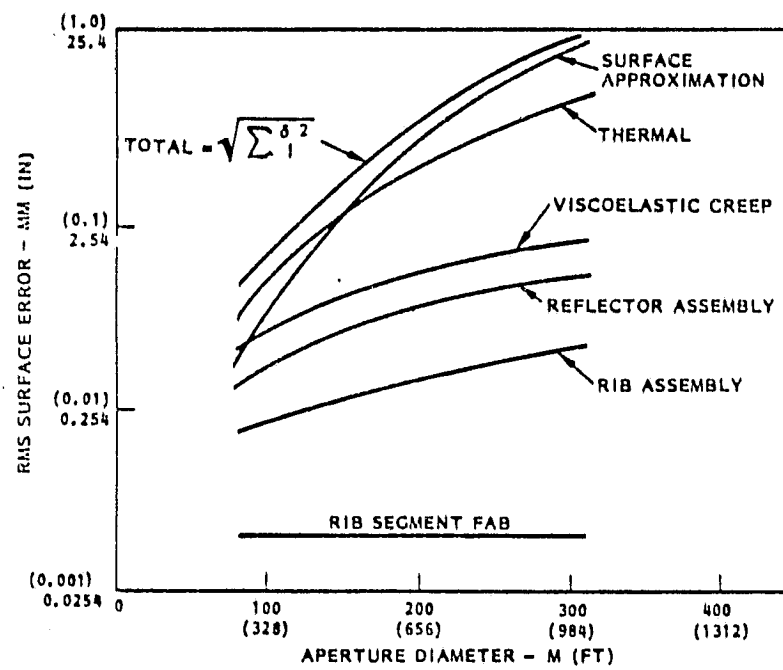


Figure 30. Synchronous P/L Surface Characteristics For a Symmetric Antenna

When the 2300 Kg weight constraint is applied to the offset antenna, the surface approximation error more closely matches the thermal distortion contribution. Comparison of Figures 29 and 30 illustrate this effect.

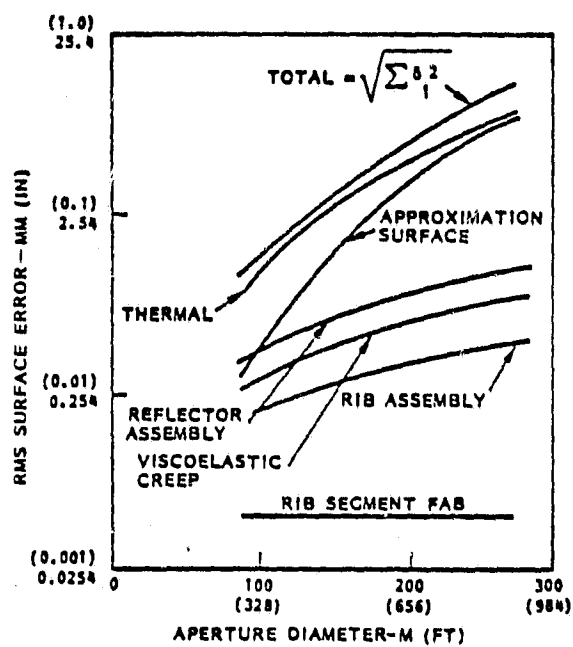


Figure 31. Synchronous P/L Surface Characteristics For an Offset Antenna

Limiting the allowable reflector weight to 680 Kg results in a surface figure that is almost totally driven by the surface approximation contribution and in fact, the thermal error became comparable to those associated with material properties and fabrication capabilities. This, shown in Figure 32, is due to the greatly reduced aperture associated with the lighter system.

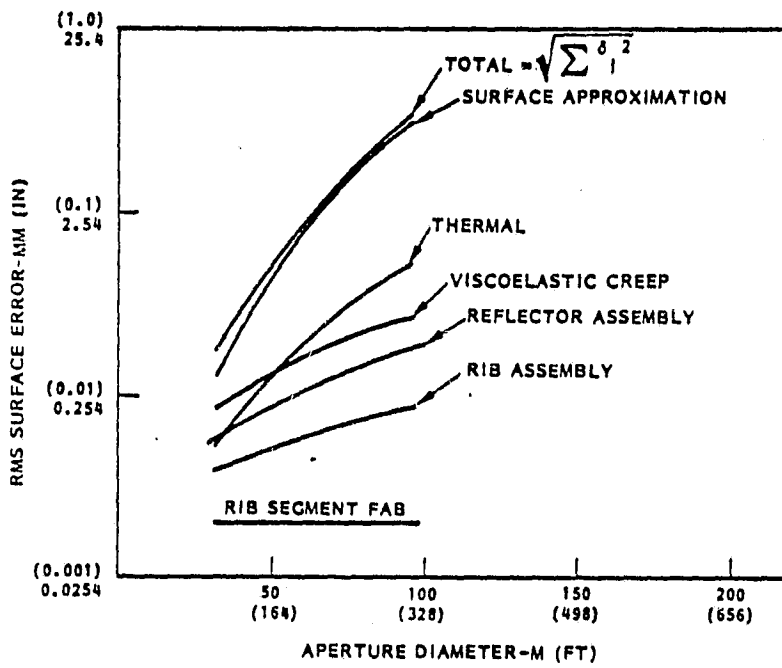


Figure 32. Synchronous Component Surface Characteristics For a Symmetric Antenna

Applying the 680 Kg limit to the offset reflector, see Figure 33, had the same effect on the error distribution as for the symmetric antenna. The effect of the higher f/D ratio can be readily seen in comparing this and the previous chart.

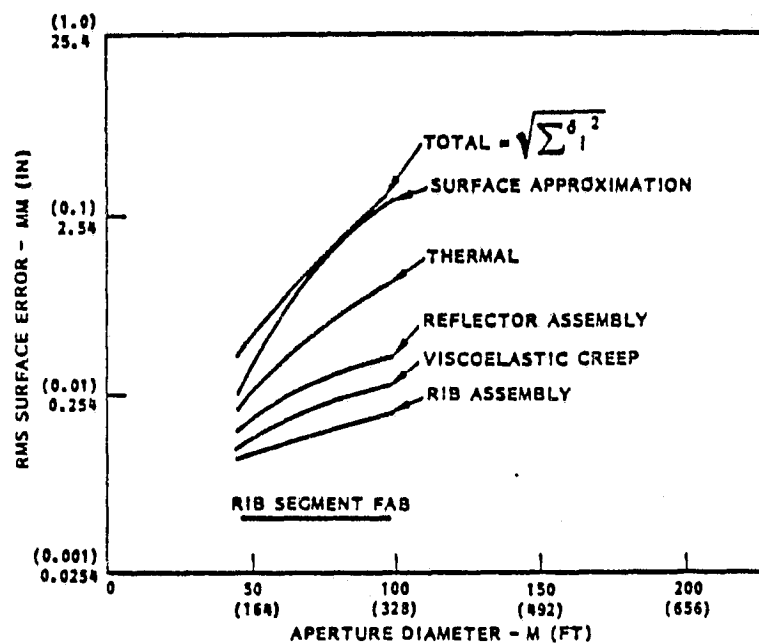


Figure 33. Synchronous Component Surface Characteristics For an Offset Antenna

### 2.3.4 Sensitivity to Design Parameters

The relationship the f/D ratio has on the frequency and aperture is illustrated in Figure 34. A given offset reflector with a parent f/D ratio of 0.25 will not perform at as high a frequency as the same reflector configured with an f/D ratio of 0.50. At a design frequency, a larger aperture can be obtained for a longer f/D ratio throughout the region of interest. This effect is present up to an f/D ratio of approximately 0.75. Beyond that, the curvature effect is no longer dominant.

The reason for this effect is due to the segmented reflector geometry. As the reflector curvature becomes less (higher f/D and flatter reflector) the effect of the flat panel approximation becomes less significant. In the limit, with an f/D of infinity, the reflector would be a flat plate and the segmented reflector would exactly approximate the surface.

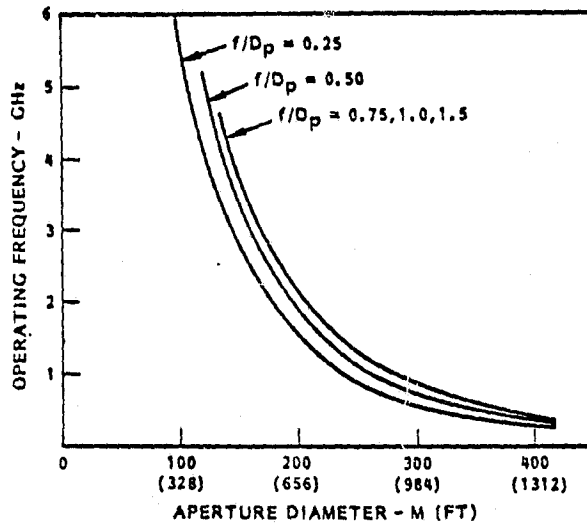


Figure 34. Antenna System Sensitivity To f/D For An Offset Antenna

Because of the impact of thermal distortion on the antenna performance, it is important to understand the causal parameters. One of the major contributors is the coefficient of thermal expansion (CTE). For the majority of the analyses performed on this study, a CTE of  $1 \times 10^{-7}/^{\circ}\text{F}$  was chosen to reflect a graphite epoxy reference structure. The performance sensitivity to this property can be seen in Figure 35.

Another property of the structure materials that has a significant effect on performance is the thermal conductivity. The advent of metal matrix composites (MMC), which combines the distortion coefficient of the graphite fibers with the thermal conductivity of metals, has had a significant effect on the projection of antenna performance.

The top curve in this figure was prepared using the properties typical of graphite magnesium MMC. The CTE used is  $1 \times 10^{-7}/^{\circ}\text{F}$  and the thermal conductivity is 18 BTU/HR -  $^{\circ}\text{F}$  - FT. The corresponding K for the graphite epoxy structure is 13.5 BTU/HR -  $^{\circ}\text{F}$  - FT.

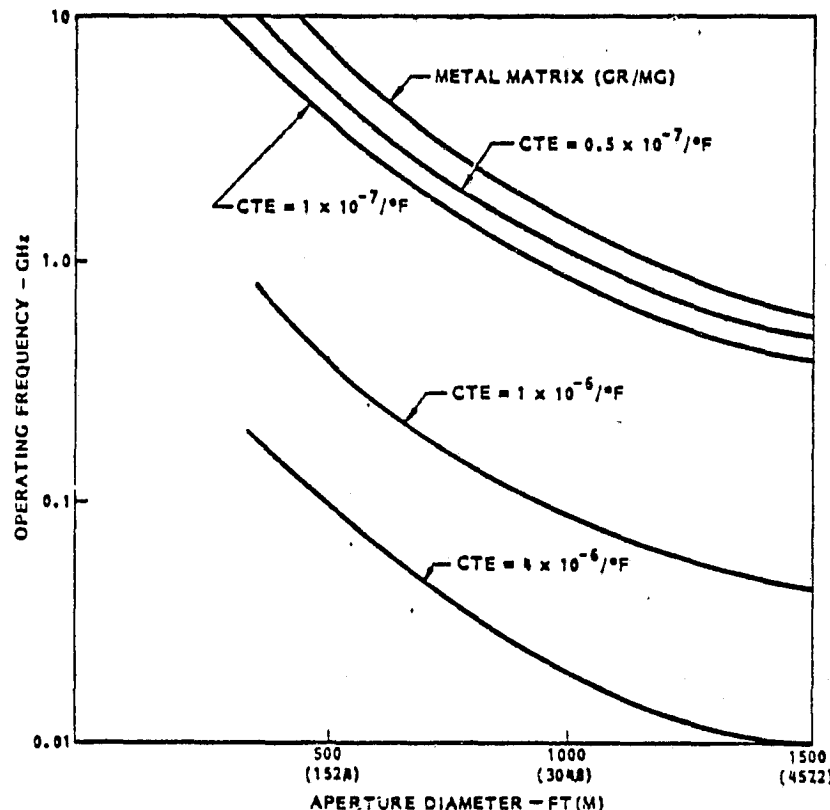


Figure 35. Antenna Sensitivity To Material Characteristics

Application of the MMC properties to the analysis of the offset reflector results in reduced surface figure errors due to the lower thermal distortion and thereby increases the useable aperture diameter at a given frequency. Note also, in Figure 36, the MMC materials will not exhibit the viscoelastic creep error associated with graphite resin composites.

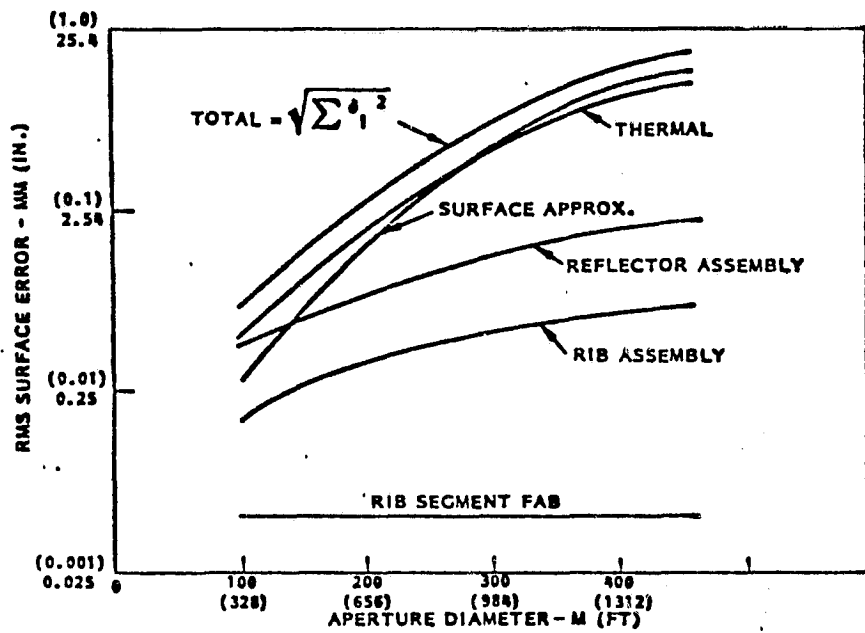


Figure 36. Surface Figure Characteristics With Metal Matrix Ribs

Throughout the analyses thus far presented, the rib configuration has been held as a constant varying only in length and parabolic shape. This lenticular rib has a hub attachment cross section (rib root) of one inch wide, four inches high and a width taper of 3:1. The effect of changing the rib root geometry to five inch wide, twenty inches high can be seen in Figure 37. Increasing the rib width and height of the rib has the effect of reducing the number of ribs that can be attached to the hub. This in turn, reduces the useable operating frequency at a given diameter and increasing the system weight. Neither effect provides a significant impact on the projected performance limits for the design.

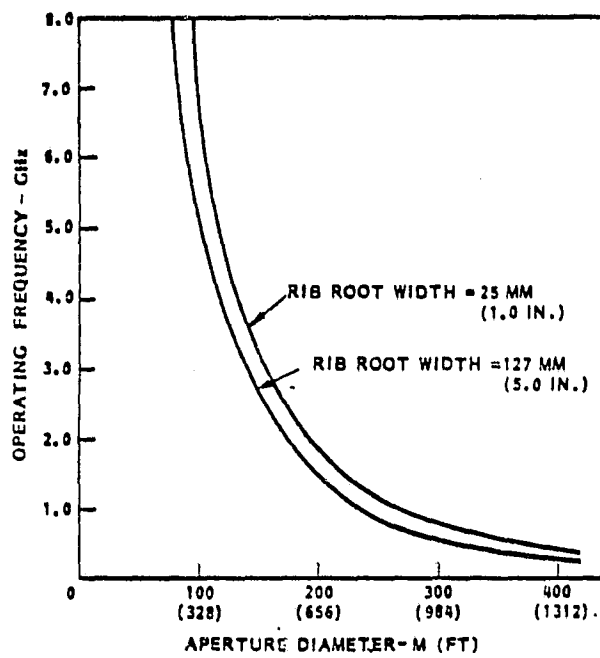


Figure 37. Antenna System Sensitivity To Rib Design

### 2.3.5 Projected Antenna Costs

Figure 38 presents the developed projected costs for an offset antenna as a function of aperture size, weight and operating frequency. The data shows that for low frequency apertures the cost is reasonably proportional to weight or diameter. As operating frequency limits are pushed the costs start to rise rapidly. This seems to occur in the 50 to 100 million dollar range for frequencies greater than 2 GHz.

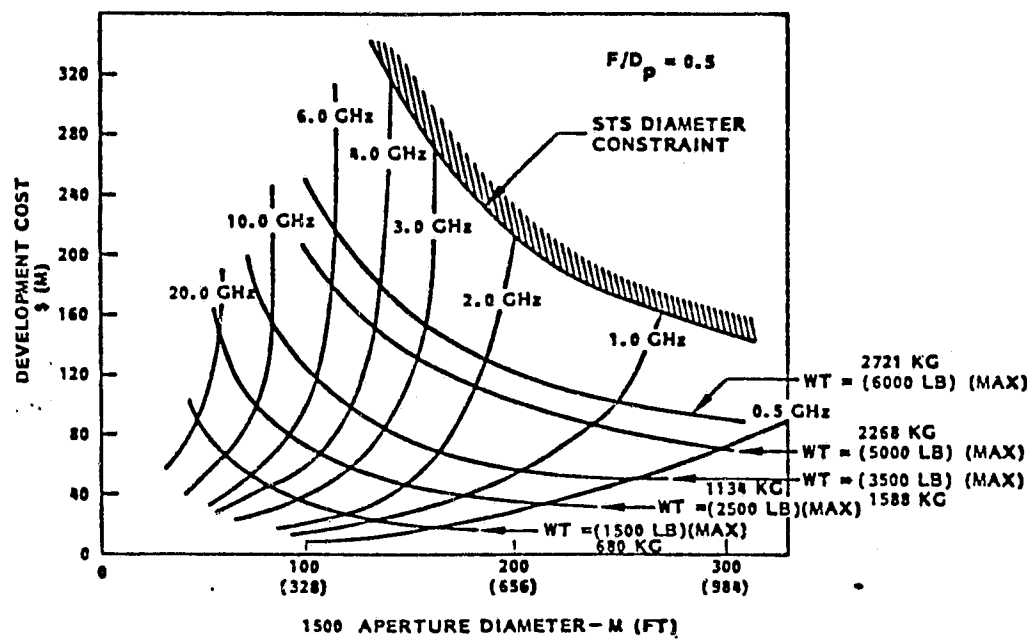


Figure 38. Offset Antenna Cost Projections

The data presented in Figure 39 presents the cost factor for an offset antenna. This increase is between 15 and 30%. The 30% factor is dominated by size and extra mast length costs while at the higher frequencies, small diameter, the costs for maintaining a highly accurate reflector surface dominates.

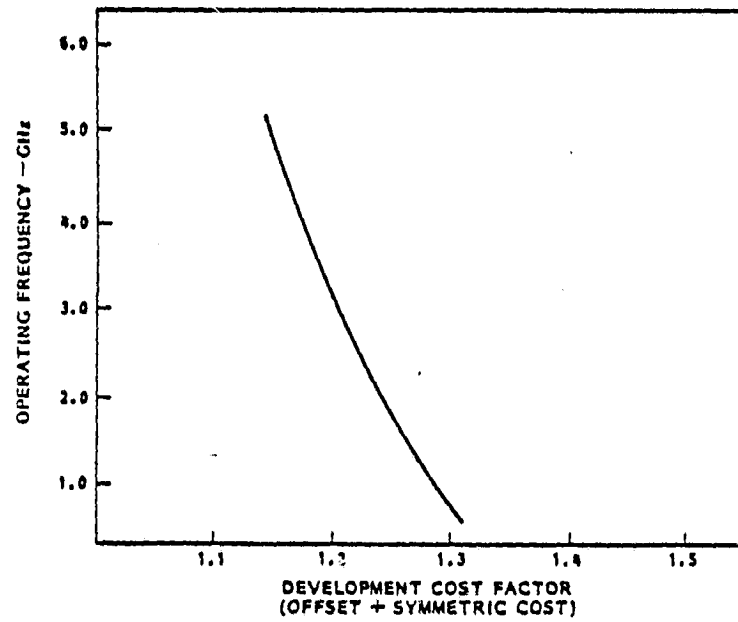


Figure 39. Offset Vs Symmetric Antenna Cost Comparison

## 2.4 PROGRAM PLAN

The data developed during the initial efforts of this study clearly indicate the potential of the wrap-rib design approach for achieving aperture sizes up to 300 m in diameter. The concerns of course with such a forecast are the limitations imposed by recognizing that the forecast is based on present knowledge. The accuracy of projecting performance over one and one half orders of magnitude must be subject to some concerns. A review of the study activity yields concern with the following items:

- o Manufacturability of Large Components
- o Assembly Alignment Facility Requirements
- o Mesh Management During Deploy/Retract
- o Vehicle Stability Requirements During Deployment
- o Lack of 1-G Testability (Contour and Strength)
- o Operational Control System Interaction/Stability

As a result of the first three of these concerns, it is felt that a new data base is required to develop the experience necessary to demonstrate confidence in the performance projections. A logical data base is afforded by a 50 to 55 m diameter reflector segment. Only by the actual production of full scale hardware can the techniques required for tooling, fabrication and assembly be developed; and only by the deployments of a full scale model can the problems associated with deployment verification in a gravitational environment be understood and solved. Therefore, the proposed program includes the design, production and deployment demonstration of a sectional model of a 55-meter-diameter wrap-rib reflector. A four rib, three gore model in which the central gore is relatively isolated from the free boundary effects will provide the best and most economic possible simulation of a complete reflector short of a full assembly.

The approach selected will provide confirmation of predicted design parameters (e.g. weight and stowed volume) as well as furnishing valuable scaling data. The selected design and the fabrication and test methods employed apply to a wide range of reflector diameters and operating frequencies. Scaling data will be directly available since rib lengths can be easily extended by splicing additional segments, and the hub/deployment mechanism method and the mesh style (opening size) can be easily modified for optimum reflectivity at any design operating frequency. All the essential technology associated with the 55-meter-diameter reflector model is equally applicable to either symmetric or offset reflector designs. Flight quality materials will be used as extensively as practical in the construction of this model.

Major objectives and goals for the engineering model construction and test are summarized below:

- o Demonstration, with a full scale working model, of the deployment characteristics of the 55-meter-diameter reflector.
- o Demonstration and verification of large reflector fabrication, assembly, and alignment techniques and procedures.
- o Verification of the durability and stability of the mesh, ribs, deployment drive assembly, and test equipment by repeated deployments.
- o Development and verification of tooling designed for rib and gore assembly fabrication.
- o Development and demonstration of stowage and handling techniques and procedures for the reflector and the test equipment.
- o Verification of the predicted packaged density of the ribs and gore assemblies.

- o Verification of the overhead support system operation.
- o Verification of the deployment envelope of the reflector.
- o Demonstration of the reflector design capability to overcome induced failure modes, including mesh and cord snags or hangups.
- o Improvement of manufacturing operations associated with the reflector and test equipment design based on the experience of fabrication and test of a full scale working model.

Most of these objectives can only be realized by the fabrication and test of a full scale working model of the 55-meter-diameter reflector.

#### 2.4.1 55-Meter-Diameter Model Design

Design features of the proposed 4-rib engineering model and test equipment are summarized as follows:

RIB ASSEMBLIES Complete assemblies including typical root section, attach fittings and 4 or 5 radial splices. Rib will be of tapered lenticular cross-section and made from GFRP.

GORE ASSEMBLIES Low stiffness mesh knitted from gold-plated molybdenum wire with adjustable cord assemblies made from Invar wire.

HUB ASSEMBLY Dimensionally and functionally equivalent to flight-type design for a 55-meter-diameter reflector. Tape rollers will be spaced as in a 48 rib reflector.

TEST EQUIPMENT      Overhead support system of fixed rails, movable carriages and balance beams. Counter-rotating turntable used to mount reflector model.

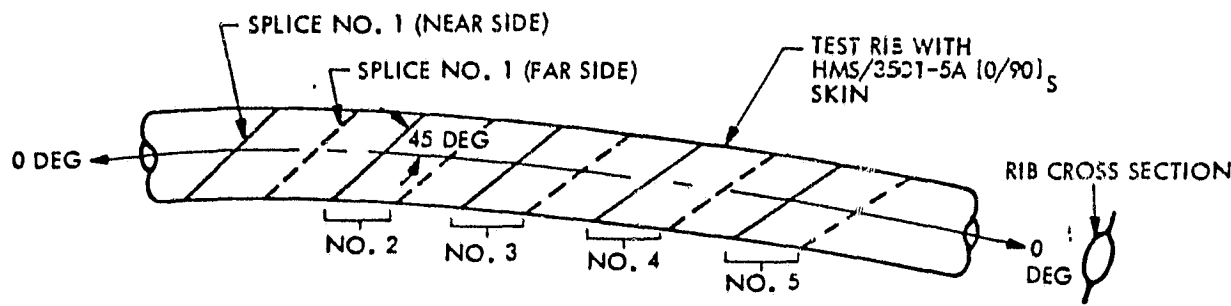
Rib and Rib Splice Design

The maximum length of a continuous rib segment is limited to approximately 6 m by the capacity of the curing autoclave construction of these very long ribs requires splices at several radial locations. These splices, however, need to be carefully designed to maintain the functional and structural integrity of the rib.

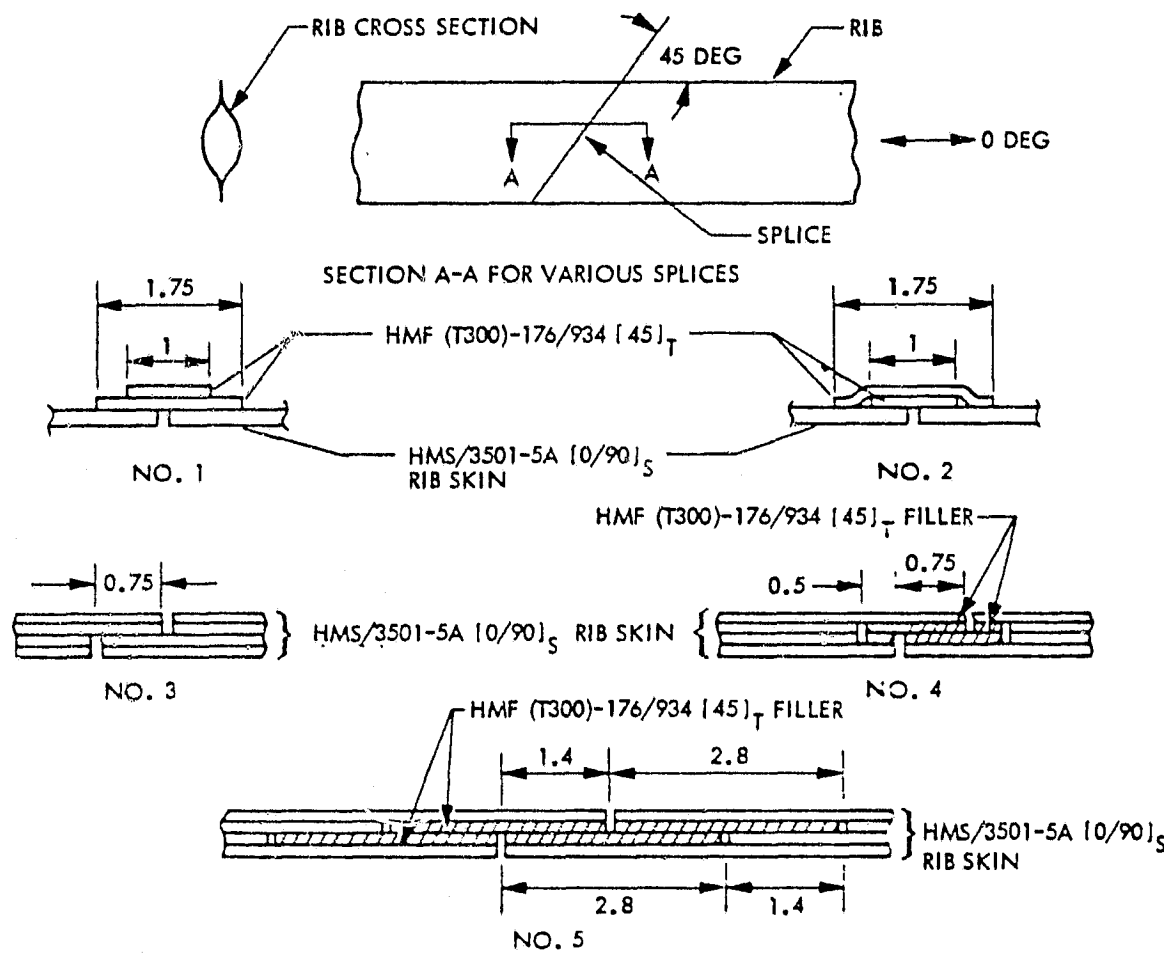
In 1979 the LMSC Independent Research and Development Program investigated methods of fabricating these splices. Analytical studies showed that splice configurations with very low flexural stiffness characteristics would minimize stress concentrations when flattening and folding the rib. These flexible splices, when positioned at an angle to the transverse axis of the rib, also localize discontinuity effects between the nonadjacent members.

Five different splice configurations were designed and tested. A sketch of a test rib containing splice candidates is shown in Figure 40 together with the construction of the splices. All candidates were subjected to multiple flexural cycles to a 0.28 m wrap radius. Splices 1 and 2 survived all tests and the rib radial splices used for the 55-meter-diameter model will be adapted from either of those designs.

The rib, which has a lenticular tapered cross section will be constructed from 3 to 4 layers of GFRP tape or fabric that will be selected based on the results of studies conducted during the initial phase of the program.



Sketch of Test Rib With Splices



NOTE: DIMENSIONS IN INCHES.

Figure 40. Lenticular Rib Splice Details

Mesh Gore Design

The reflective mesh that will be used for the 55-meter-diameter reflector model was developed by LMSC during 1978 under Independent Research and Development funding. This mesh (Figure 41) is a two-bar tricot knit produced by Continental Warp Knits, Angler Division, on a 168.0 inch wide tricot machine specially modified and used exclusively for knitting fabric from fine wire. Goldplated (6% by weight) 1.2-mil-dia molybdenum wire is obtained from Sylvania. Mesh opening size is approximately 9 mm by 9 mm when preloaded to the design value.

Cord assemblies will include fittings at each end for attachment to the rib, and adjusting turnbuckle and a small (0.005) diameter Invar wire that spans two adjacent ribs. Approximately 30 cord assemblies will be used in each gore, spaced 1 m apart along the rib surface. The cord assemblies in a gravitational environment, depress mesh pillow by increasing chordal and radial load ratio in the surface; allow post-assembly adjustment of surface loads; and produce a preloaded, thermally invariant, orbital contour. Since the stiffness of the cord assemblies is much greater than that of the mesh, the reflector performance is nearly independent of mesh preload and is insensitive to uncertainties in the mechanical properties of the mesh. The cord assemblies will be made from drawn and annealed Invar-36. Each of the four edges of the gore assembly will be terminated by bonding to a Kevlar-47 fabric strip approximately 6.35 mm wide by 0.13 mm thick.

2.4.2 55-Meter-Diameter Reflector Test Equipment

The reflector model ribs will be supported by a system of test equipment during furling and deployment operations. This test equipment will be a passive overhead support system that progressively offloads the weight of the ribs and mesh as they are unfurled from the central

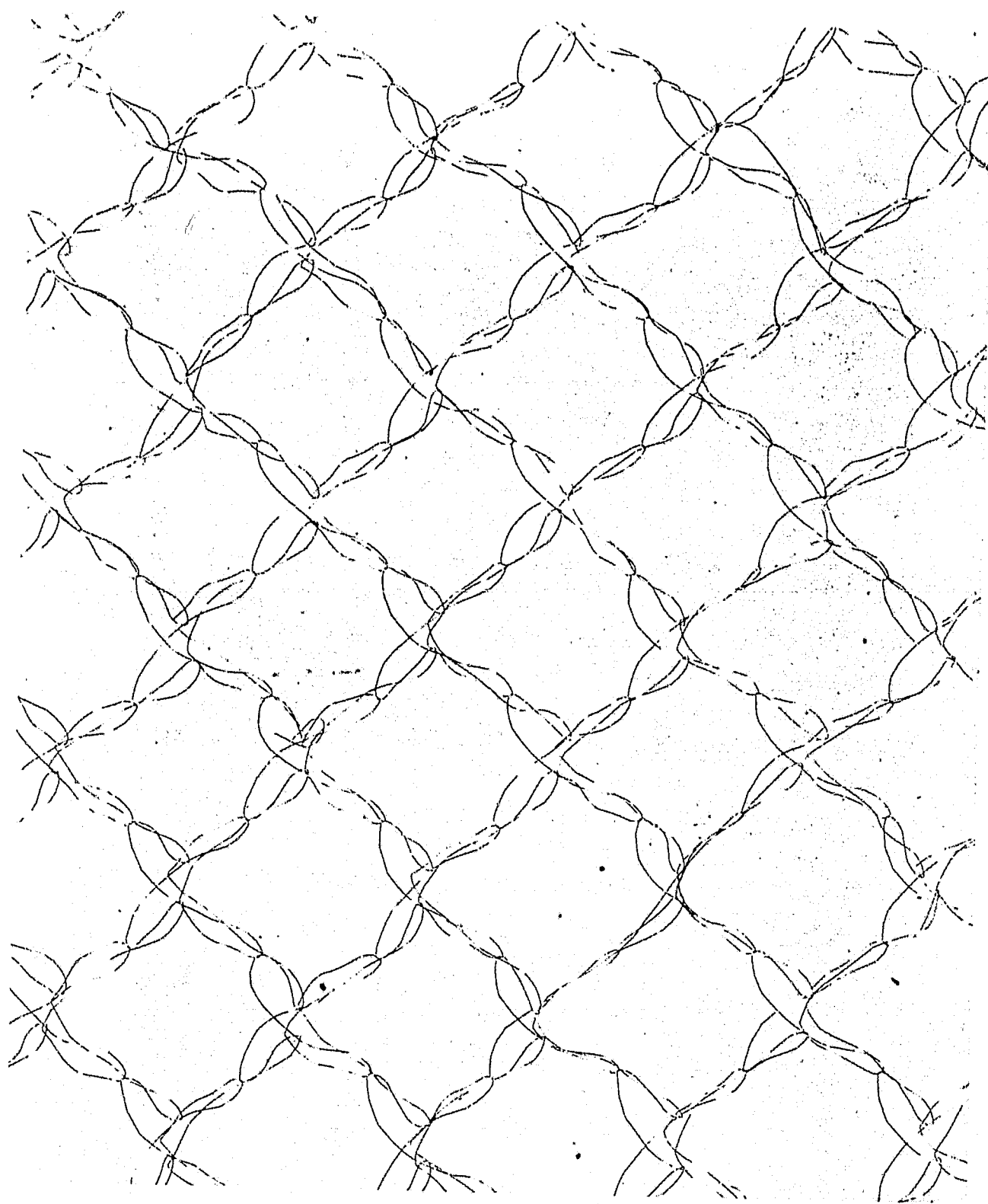


Figure 41. Gold Plated Molybdenum Wire Mesh

hub mechanism. The test equipment will consist of four fixed overhead support rails on each of which, four sets of balance beam/carriage assemblies will ride. These balance beams will be attached at predetermined positions during the deployment.

The natural motion of the ribs will be tracked by the carriage assemblies in the radial direction and by the balance beams in the vertical and lateral directions. To maintain the rib positions approximately colinear with the overhead support rails the hub will be mounted to a platform that rotates opposite to the direction of ring that moves the deployment tape assemblies.

This simple, passive overhead support system that provides three degrees of freedom offsets gravitational forces and moments during deployment and will support the deployed model in such a way that distortion of the parabolic shape is minimized.

#### 2.4.3 Reflector Model Fabrication and Assembly

Manufacturing of the 55-meter-diameter model ribs will require the fabrication and assembly of right-hand and left-hand GFRP rib segment halves. Rib halves will be bonded to form the lenticular cross-section and then mated to the root attachment.

Tooling for the layup, bonding, alignment, and assembly of the ribs will be machined from aluminum plate. Engineering drawings generated by computer aided drafting techniques will be used directly to create numerical control tapes for machining the mold surface into aluminum tooling plates. These individual layup tools will also be used as rib assembly tooling during the splicing assembly operations. NC witness points will be machined into the tool to facilitate alignment and inspection.

The model surface will consist of three gore sections measuring approximately 27 m along the two long sides and approximately 3.6 m opposite the apex. Gore sections will be fabricated from a single piece of gold-plated molybdenum wire knitted fabric. A flat pattern layout of the gore and cord lines will be located on a load table. A uniform pretension will be applied to all four edges of a rectangular panel prior to cutting it to analytically predetermined dimensions. Rubber strip magnets will hold the cut gore as the Kevlar edge strips are bonded in place and the presized cord assemblies are woven into the gore. The gore will then be folded and rolled onto a large spool for storage until final assembly to the ribs.

Each of the ribs will be attached to the hub by suspending it from the overhead support rails and attaching it at its root to a fitting mounted on the hub. The overhead test equipment will be substituted for the temporary lifting lines. Each of the remaining ribs will be installed in succeeding order. When all four ribs have been installed and fastened to the hub they will be furled. A rib-only (without mesh) deployment will be performed to verify functional operation of the hub and rib assembly before installing the mesh gores.

The gore installation is initiated with the ribs furled on the hub. Starting at the tips, the gores will be attached to the ribs as they are deployed outward. The previously fabricated gore assemblies, contained the reinforcement cords, are payed off of their larger storage spools as the ribs are extended. When the ribs are completely deployed the final assembly is complete and packaging and deployment testing will begin.

#### 2.4.4 55-Meter-Diameter Reflector Model Implementation Schedule

The implementation schedule for the design, production and test of the four rib 55-meter-diameter reflector model is shown in Figure 42. A

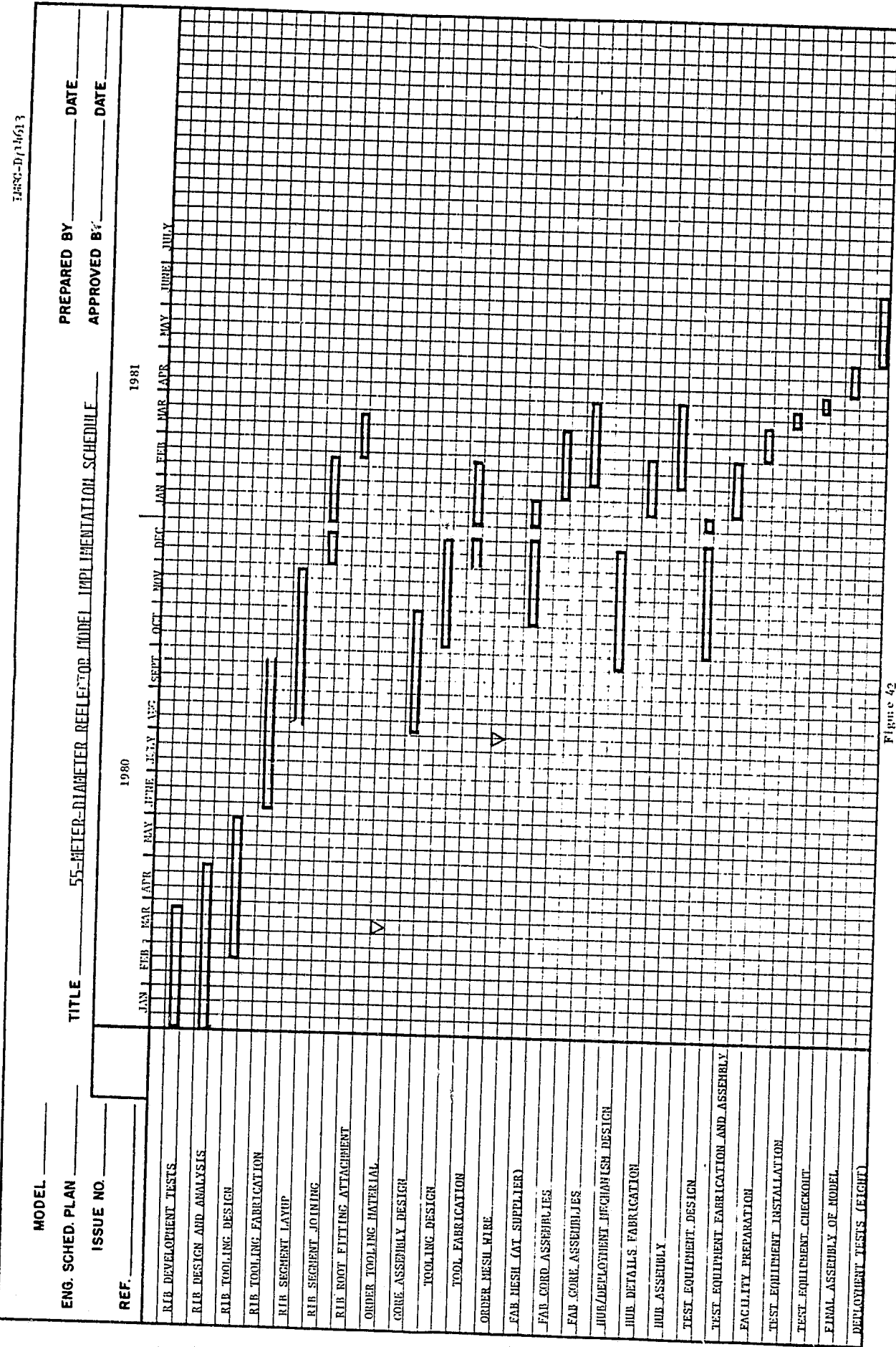


Figure 42

start date of January 1, 1980 has been used. Program completion is indicated as July 1, 1981 producing a program duration of 18 months.

Early activities, initiated at start of contract, are primarily associated with rib design, analysis, and component development tests since rib production represents the longest and most critical element of the schedule. These analyses and tests must be completed during the first three months of the program in order to support the rib tooling design effort. Rib component development tests will include coupon level strength measurements of the selected GFRP material and layup, short (approximately 2.5 m) beam tests to verify rib wrapping characteristics, and demonstration of the selected splice and root section designs. Analytical studies will include strength analyses of the rib (splices and root section), deployed stability analyses, mesh and cord preload optimization and calculations of rib and gore dimensions required for tooling design.

Rib design documentation will be in the form of CADAM produced drawings so that numerically controlled milling machine tapes may be made directly from design drawings. An order for sufficient tooling material (recast aluminum) must be placed during the first quarter. This material will be delivered to CALAC where the 10 separate rib layup tools will be machined. Layup and cure of the segments will be accomplished in the LMSC composites manufacturing facility using an existing 24 foot capacity autoclave. Segment joining (rib assembly) will also be done in the composites fabrication area.

A critical milestone in the production of the gore assemblies is the placement of the gold-plated molybdenum wire order with Sylvania. This wire is delivered directly to Continental Warp Knits where it is knitted into a continuous piece sufficient to fabricate the three gores. The major tool associated with the fabrication of the gore assemblies is a large table on which the rectangular mesh panels are pretensioned, cut,

<sup>69</sup>  
PRECEDING PAGE BLANK NOT FILMED

and fitted with edge terminating strips. Construction of this table will be completed by mid February 1981. Assembly of all gores will be completed by the end of March 1981 and available for installation on the model.

The hub assembly, which includes the spool and tape deployment mechanism, will be completed and functionally tested before the end of March 1981. Reflector model final assembly will begin at that time.

A facility of suitable dimensions (approximately 55 feet high, 100 feet long and 50 feet wide) will be available by early March for installation of the overhead test equipment.

Six weeks have been allocated for the performance of the eight scheduled deployments.

### SECTION 3 CONCLUSIONS

The activities performed in support of this study clearly indicate that the wrap-rib reflector approach toward achieving large apertures in space is a viable candidate. A detailed analysis of the design indicates that diameters of 150 to 300 m are possible. These apertures exhibit characteristics which will allow operation at frequencies in the 1 to 3 GHz region. It was further determined that adapting the concept to an offset geometry antenna is not only feasible but allows the concept to be extended for additional performance in either frequency or diameter. The mast configuration developed has been shown to be compatible with both the STS constraints and the antenna thermal stability requirements.

The cost algorithm results indicate that the large apertures are going to be expensive if pursued to the limits of technology. However, the results also indicate that the technology impacts on cost do not become a major driver until 150 m in diameter is exceeded. At 150 m in diameter a 2 to 3 GHz reflector is forecasted to have a cost that is reasonably dependent on the system weight (ref. Figure 42) and not driven by manufacturing and assembly precision as indicated by the slope of the cost growth curve.

The ability to forecast technology growth over one and one half orders of magnitude must be questioned. Therefore the final conclusions should be conservatively stated and reflect these scaling concerns.

These restrained conclusions are as follows:

- o Offset wrap rib antennas up to 150 m diameter are feasible for operation at 2 to 3 GHz.

- o STS compatibility is not a design driver.
- o Cost and technical risks indicate a new data base required prior to undertaking 100 to 150 m designs.
- o Further activity should include active surface control and control systems interaction studies.

## SECTION 4

### RECOMMENDATIONS

The results of the investigation were surprising and satisfying. Projections indicate the appropriateness of the Wrap-Rib for large diameter antennas. Technically however, there are concerns which must be addressed prior to a development program undertaking. The projected costs and technical risks indicate the necessity of developing an early data base at a size which could comfortably be analytically scaled and which would reduce risk through demonstration. This program, identified below, would involve developing a testable segment of a 50 m aperture. This would be used to validate the design and provide a scaling factor of 2 or 3 for the 100 to 150 m missions. The dominant effects of thermal distortions in the performance projections indicate orbital surface adjustment may prove cost effective and should be investigated. Finally, since the design is being defined the stability and control system interactions and limitations should be identified.

#### ESTABLISH A COST EFFECTIVE 50 M DATA BASE

- MANUFACTURE AND TEST COMPONENTS/PROCESSES
- ASSEMBLE I-C TESTABLE SEGMENT
- DEMONSTRATE DEPLOYMENT AND RETRACTION
- MEASURE DEPLOYED CONTOUR WITH OFFLOADING TEST AID
- UPDATE DESIGN AND DESIGN ALGORITHM

#### EVALUATE BENEFITS OF INCORPORATING ACTIVE FIGURE CONTROL

- ONE TIME ADJUSTMENT
- CONTINUOUS ADJUSTMENT
- DEGREES OF FREEDOM REQUIRED
- COSTS

#### INVESTIGATE CONTROL SYSTEM INTERACTION

- DEFINE PRELIMINARY REQUIREMENTS
- INVESTIGATE ACTIVE DAMPING AND DISTRIBUTED CONTROL SYSTEM

SECTION 5  
NEW TECHNOLOGY

There were no applicable new technology items identified during the conduct of this study.